A "quantum network" theory to model, design and operate a district's energy systems

Malick Kane[a*], Lucile Schulthess[a]

School of Engineering and Architecture (HEIA-FR), Mechanical Engineering Department,

HES-SO // University of Applied Sciences and Arts of Western Switzerland, Boulevard de Pérolles 80,

CH-1700, Fribourg, Switzerland, +41 (0)26 429 68 42, malick.kane@hefr.ch

Jérémy Rolle[b],

Groupe E Celsius SA

Route de Chantemerle 1, CH-1763, Granges-Paccot, Switzerland,

+41 (0)26 352 68 46, jeremy.rolle@groupe-e.ch

Abstract:

New generation District Heating/Cooling (DHC) systems are more complex and difficult to simulate, design and operate. The cluster or layer-based design method consists of dividing a large network into multiple subsystems (clusters, layers or sublayers). Compared to old modeling and design methods, it is better suited to simplifying simulation without any loss of information on the network system and to integrating optimization with several design options. The simulation of clusters or layers and the connection between them still require iterative procedures – a very time-consuming optimization process (with or without algorithms). An original and alternative method of cluster/layer-based design modelling inspired by "quantum mechanics" is proposed for the simulation of complex networks with no iteration procedures. It consists of representing any network, cluster, layer or sublayer in an equivalent branched network called a "quantum network". Based on this theory, the distribution of energy in the quantum network can be expressed by using quanta (distribution of energy on the basis of discontinuous quantities). Quantum network energy is defined as the minimum quantity of flow energy to be transferred in a network's system or subsystem and is given

as a constant multiple (k_0) of a simple quantum state function ($\bar{v}$). The latter being characteristic of the system. Such a "quantum flow-energy" formulation is implemented in the "ADVENS" network simulation tool and used to simulate the performance of various district energy systems. In this study, we present, step by step: i) the discretization methodology as well as the detailed quantum network's energy models; ii) the process on how to convert an existing/real DHC network into a "quantum network" and iii) the approach on how to formulate an optimization problem using "isotopes" to simulate systems with several examples of network configurations. The validation of this method is done: a) first by comparing results with simulated data from a well-known commercial software (Neplan). A relative error between 0.8% and 2% is obtained for all parameters, like temperature, pressure, mass flow and heat-rate; and b) by calibrating models with real data from existing/operating networks (low and high temperature networks). A great simulation results accuracy with a deviation in the order of 1% is obtained in winter and between seasons. However, in summer, the input data of the model, in particular the hourly load scenarios for domestic hot water (DHW) production, are not fully validated. The deviation is in the order of 5% for a thermal load between 5-16% of the nominal value.

Keywords: District heating, Energy systems, District heating/cooling networks, Methodology modelling simulation

Nomenclature

Acronyms

COP	Coefficient of performance (heat pumps)
DH	District heating
HP	Heat pump

SST Substation

Symbols

A segment number, mass number, -

c_p specific heat, J/ (kg K)

D diameter, m

f friction factor, -

h heat transfer coefficient, W/(m^2K)

k sublayer quantum number, -

k_0 Mean Capacity Constant of the quantum network, W/K

l Secondary quantum number, -

L length, m

$\dot{M}$ mass flow rate, kg/s

m number of electrons bounded to the layer or sublayer, -

n primary quantum number, -

P pressure, Pa

q energy load, -

$\dot{Q}$ Heat rate, W

r radius, m

T temperature, K

U overall heat transfer coefficient, W/(m2K)

v velocity, m/s

X atomic element, -

$\dot{Y}$ quantum flow energy, [W]

$\dot{y}$ quantum flow energy per unit of mass, [W/kg]

Z atomic number, -

Greek symbols

Δ difference

δ specific or relative temperature difference

ε effectiveness, -

μ quantum flow number, -

ν quantum state function, [K]

λ thermal conductivity, W/(m K)

τ thermal-hydraulic dimensionless factor, -

ρ mass density, kg/m^3

Subscripts

0 in relation to source

a ambient or reference

e electron

i source side of a pipe

f substation side of a pipe

l linear, branch (or layer)

o outlet

p proton

s supply, segment (or sublayer)

r return

1. Introduction

During these last few years, existing district heating (DH) networks have expanded and an increasing number of new ones have been built. They have emerged as a promising solution to reduce the primary energy consumption required for buildings [1], [2]

Historically, the first generation DH appliances were built to serve urban neighborhoods by recovering heat from industrial or incineration plants [3]. They were therefore sized for high, or even very high, temperatures. From that point on, DH temperature has consistently diminished since this kind of appliances is more efficient when operating at lower temperature levels. The new generations DH is increasingly used with cogeneration and/or with combined heating and cooling. 5th generation district heating/cooling (DHC) systems integrate the smart thermal grid, since, compared to previous generations they can efficiently use renewable energy sources [4] [5].

Today's DHC systems are more complex and difficult to design and operate, for different reasons. The number of consumers and producers are increasing and can be operated in heating or cooling mode with different energy sources. Some houses are self-consumed during the summer, thanks to solar panels. To increase the system's reliability, networks are interconnected, expanded and contain loops and bidirectional pipes. In addition, they use multiple sources and become interconnected with networks at different exergy levels. For example, low temperature networks (5th generation district heating with decentralized heat pumps) require pairing with the electricity network for a smart inclusion of HP [6]. These networks become more challenging to model and simulate, and their design and operation optimization is time-consuming because of a large number of iteration procedures.

In this study, an original method inspired by "quantum mechanics" is described and used for modeling and simulating complex networks with no iteration procedures. The ADVENS network simulation tool developed by the Laboratory for Thermal Energy (LTE) systems at the Swiss University of Applied Sciences of Western Switzerland (HES-SO) integrates this methodology. It is a new tool that can be used by engineers to evaluate networks' performance, both in an early conceptual design phase

– through an optimization process – or in a detailed design phase and/or for an existing network in operation.

1.1 Current methods for thermal networks modeling and simulation

A thermal network uses a heat transfer fluid (HTF) or a refrigerant in pipes to distribute the flow of energy produced by one or more heating/cooling plants to different users (a district, a town, an industrial zone, etc.). Thermal networks are very diversified in size, power and efficiency. They allow the centralization of energy production in order to optimize the overall efficiency of district heating/cooling (DHC) installations. Depending on the fluid and the layout of energy substations, several types of network structures can be identified: branched networks, meshed networks and mixed networks. Figure 1 shows two variants of branched and meshed network structures. In the case of a branched network, the path that connects the power plant to the user is unique. In the case of an intervention between these two points, the user will no longer have access to the energy distributed by the network. In a meshed network, there are several possibilities of supplying energy to substations, which can be an advantage, as this type of network can have several energy sources. There are also other types of networks that are rather mixed because they have a “master loop” on which small branched networks are connected.

Figure 1: Schematic representation of two kinds of network's connection. a) Branch network with one source and three substations (consumers). b) Master loop or merged network with one source and three substations (consumers)

Most of the times, thermal network pipes are arranged in pairs (supply and return pipes) that have the same path. Consequently, a topological description of a thermal network can be obtained just by

drawing a line to specify a so-called branch of the network. The other network equipment or components are simplified as nodes (or junctions)

With the branches/nodes formulation, there are four different methods for modelling and optimizing a DHC system with unknown or predefined parameters: loop, node, pipe and mixed node-loop methods [7]. The loop method uses the corrective mass flow rates as unknown parameters – a method especially used for hydraulic analysis. The nodes are connected by lines based on the graph theory [8], [9] [10]. Figure 2 shows an example and model of a loop network graph. In the nodal method, the unknown parameters are the pressure heads at nodes (junctions). Some models rather use pressure drops. These models are inspired by the electricity law and Kirchhoff's circuit laws and apply a pressure balance to the nodes [11]. For the pipe method, the unknown parameters are the pipe mass flow rates.

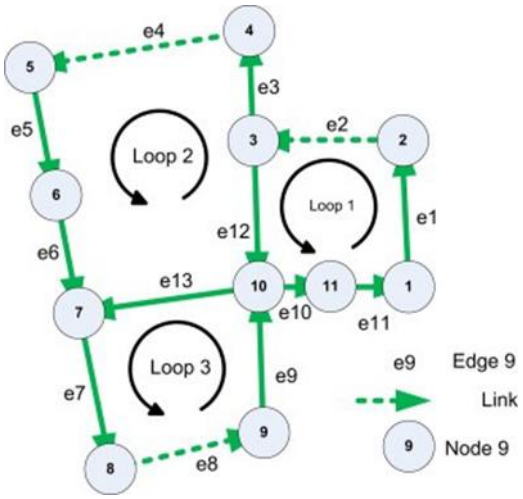

Figure 2: Network graph model [4]

These different methods, based on a branch/node formulation, use an iterative procedure to solve the system because the nonlinear equations complicate the resolution and any optimization process (a simulation model coupled with an optimization algorithm) is complex, difficult and time consuming. Other existing models use experience and data to reduce the predefined parameters or to consider the knowledge in the secondary circuit (energy consumer circuit). For example, some models are based on an Artificial neural network. The code is a succession of layers, each taking its inputs from the

outputs of the previous one. They have the possibility to map linear and non-linear relations and solve complex problems. However, the definition of all functions is very long and tedious [12], [13].

Another strategy to reduce the complexity is to use aggregation methods. Figure 3 shows two main models of aggregation methods. All the nodes are collapsed to one line [14], [15]. An equivalent network system is calculated to have a correct resolution. The main advantage of these methods is the low processing time needed to find the solution [16]. However, the network is systematically simplified with detailed information loss on the network. The smaller branches are merged with bigger ones and only the transport circuit is calculated, while the distribution circuit is avoided. Such aggregation methods can be used as a first approximation in a design process and models cannot be generalized for any network systems.

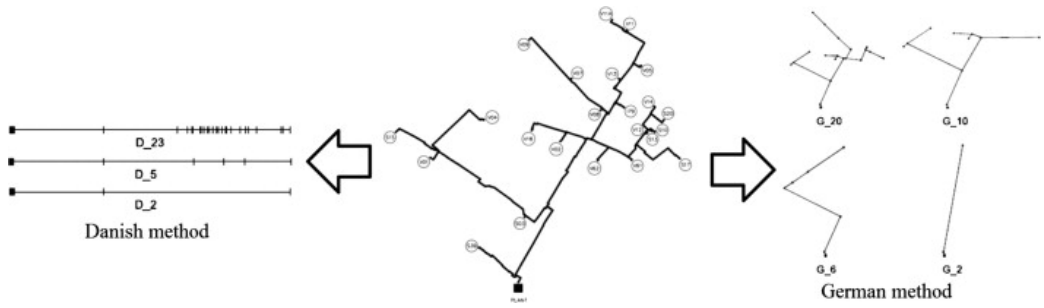

Figure 3: Aggregation method with two main models from the publication [11]

Another simplification method without loss of information on the network system is the Cluster-based design. Figure 4 illustrates the clustering model. The area is divided into multiple small distribution clusters or subsystems. They are connected with distributed substations. Each cluster is resolved independently. The resolution and optimization of the first distribution network is easier [17][18].

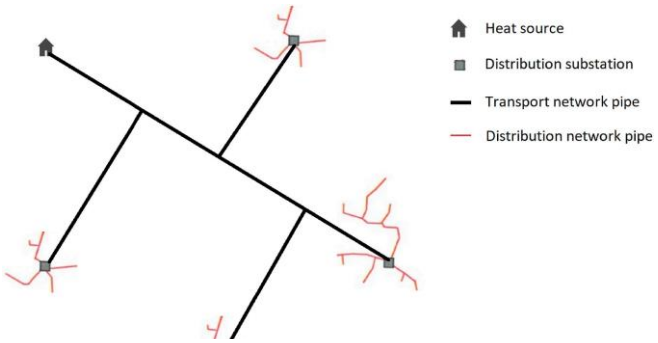

Figure 4: Cluster-based design from the publication [14]

Following the same idea, the simulation with two (or more) layers can also be performed (Figure 5). This model creates layers and run them in simulations independently, in the same way as for the cluster-based method.

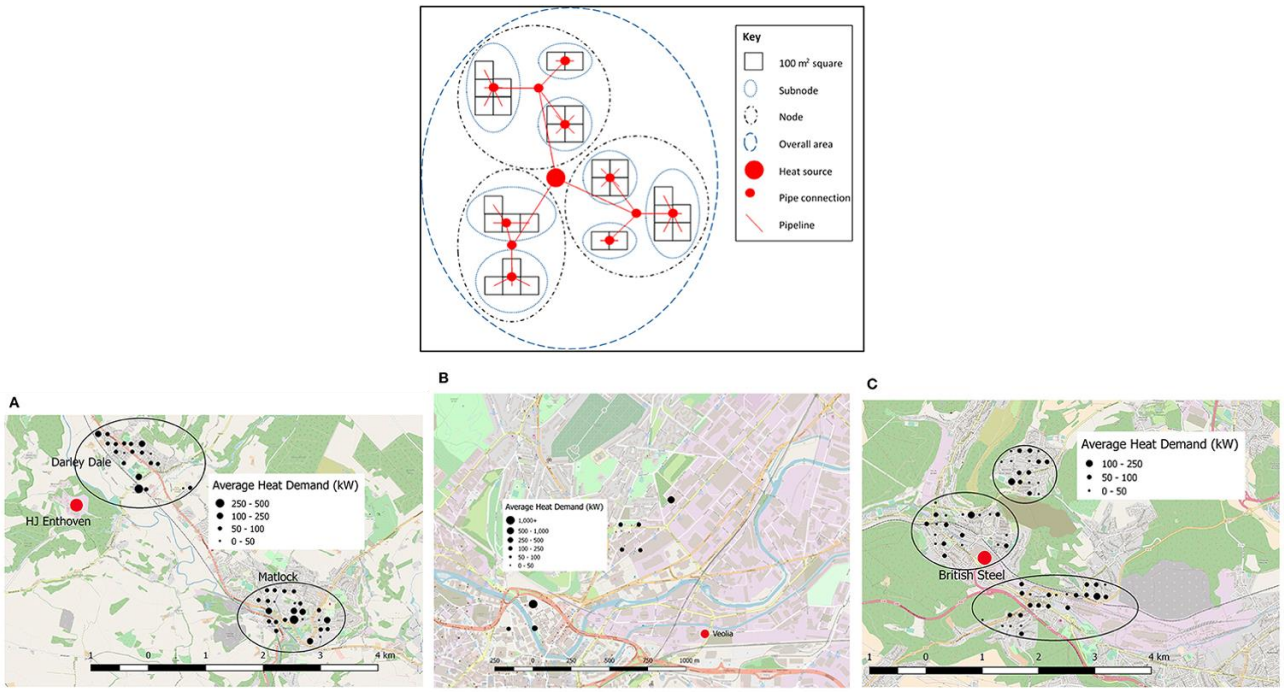

Figure 5: Archetype method illustration from the publication [16]

Most of these cluster- or layers- based design have an optimization strategy which consists of simply comparing several design options with no real use of algorithms or a multi objective optimization with the example of using genetic algorithms [20], [21] or with the ability to process big data [19]. However, the simulation process of clusters or layers and the connection between them remain to be performed by iterative procedures.

A new approach to Cluster-based design modeling is carried out according to the quantum network discretization methodology described by (Kane and Rolle, 2020) and applied by (Yolaine and all, 20xx) to simulate the BlueFactory network system. It makes it possible to avoid iterative procedures and to represent any type of network in an equivalent branched network called a “quantum network”. The following presents, in more detail, the discretization methodology, the flow, temperature and pressure distribution models as well as the “quantum flow energy” formulation used to simulate, design and operate district energy systems. With a view to applying this method, we’ll show its benefits by showing step by step how to convert existing/real district heat/cooling network into a quantum network and how to formulate the optimization process to compare different systems with a variety of network configurations. The validation of this method will also be done by comparing results with simulated data from a well-known commercial software (Neplan) and also by using operating data from existing networks.

2. A new approach to Cluster-based quantum network design

This method uses a specific terminology to describe a DHC network system. The network is composed of a main transport (or primary) circuit that includes divergents to separate the flow and tees to connect substations (SST) through a distribution circuit. Figure 6 shows an example of a simple DH network system in which the primary circuit is composed of one divergent and three different branches. Each branch can be split into different segments (e.g., a part of a branch that supplies a substation). Thus, a branch includes all parts of the system that are directly between a source and a divergent, between two divergents and between a divergent and an end-valve.

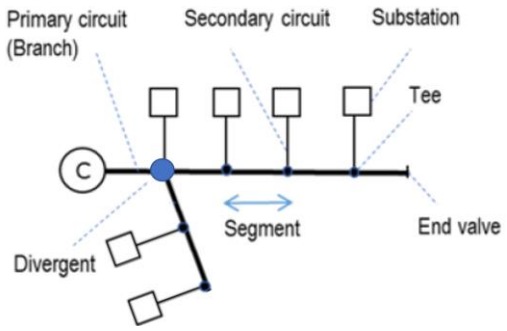

Figure 6: A network graph, showing 1 Source, 1 Divergent, 3 branches, and 6 Substations

The primary circuit has a main source, namely the central (C), which produces the required energy for the DH. The transport/distribution network provides the amount of energy necessary for customers to used it. SSTsdiver transfer energy from the DH to the consumer, generally through heat exchangers or heat pumps for lower temperature networks. Consequently, SST generate a temperature difference between the inlet and outlet of the network distribution circuit. SST can also be a source of energy. For example, in thermal smart grids, other decentralized plants (or distributed supply energy units) can be installed in the network. Thus, SST can be consumers (sinks) and/or producers (sources) depending on the conditions (for example, a building using both heat exchangers for heating purposes and solar thermal collectors to supply solar energy to the network).

In the case of a loop or primary circuit with multiples branches, a divergent and a convergent are used for distributing the flow.

Though essential in DH, the pumping system is not shown in the diagram. Several cases can be differentiated: a centralized pumping system that has only one pump to deliver the fluid to the source, the network and the substations; or a separate pumping system specific to the primary circuit and another that is specific to the secondary circuit. Two strategies can be used to provide energy to SST: either the flow rate is constant, which implies that the pumping energy is constant; or the flow is variable, in which case the thermal power and consumption of the network can be more easily adapted (smart network). Modern DH systems are typically operated using a variable flow.

A district heating/cooling network, though quite complex, can be subdivided in one or more elementary-network subsystems. Each elementary network is considered as a Cluster that can be

simulated separately with its own equations. A cluster may contain divergents and/or convergents, tees or substations or any other energy source or sink equipment. It is defined by the amount of its energy conveyed in the network; its efficiency; its temperature and pressure levels and the characteristic sizes of the branches and segments that supply its substations. The cluster can also contain branched or meshed circuit elements. A quantum network energy formulation will make it possible to model and simulate the distribution of energy in simple or small networks, as well as in larger, multi-source energy networks featuring many substations with different exergy levels.

2.1. The quantum network discretization methodology and terminology

2.1.1. Notion of quantum network based on atomic elements

The quantum network theory aims to use some similarities with quantum mechanics to consider the Cluster as an aggregate of particles (such as atoms, neutrons, protons and/or electrons) in direct interaction with each other, with their links, layers or sublayers (branches or segments). The level of energy of any particle is quantified and depends on their position in the system and also the distribution of energy in the branches and segments.

Based on this formulation, the cluster is formed by a nucleus (primary network system components) and electrons in the distribution network. The nucleus includes two types of nucleon particles: The protons (p) represented by the tees, which are located at the starting points of the distribution circuit; and the neutrons, (n) represented by the divergent located at the primary circuit. Electrons (substations) are connected around the nucleus. All clusters are made up of these three types of fundamental particles. The number of protons, also known as the atomic number (Z), is also equal to the number of electrons. The mass number (A) represents the sum of the nucleons (n+p).

Next to A and Z, the symbol X is used to denote the atomic element (${}^{A}_{Z}X$). Figure 7 shows the elementary network cluster according to the above elements.

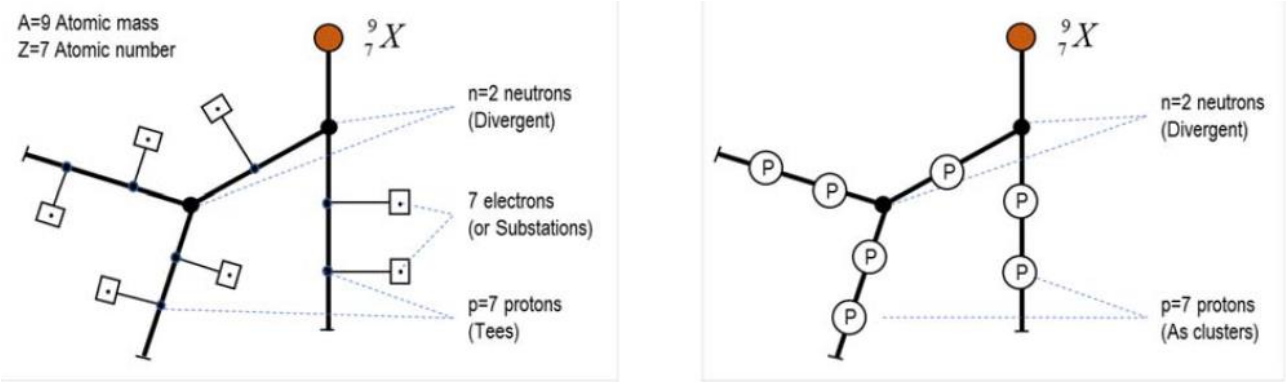

Figure 7: Representation of elementary network clusters (a) Detailed elementary network cluster (b) Atomic network cluster with Protons (P)

In Figure 7, the nucleus of the atom consists of p=7 protons and n=2 neutrons, giving an atomic mass A=9 (which represents the number of protons and neutrons). The atomic number Z=7 (the number of protons and by extension the number of electrons), and the mass number A designate the cluster or atomic element X. In the case of an atom consisting of a single proton, i.e. Z=1 and A=1, the element $^{1}_{1}X$ is designated by a proton, $^{1}_{1}P$. Figure 7 shows another way of representing the network by replacing the substations with atomic elements P (in this case, the secondary circuits are not represented). A network cohesion is directly related to the type of connections (links) between its particles (neutrons, protons and electrons). Two main families of links exist: the primary links (segments with higher flow rate), which involve neutrons and protons; and the secondary links, internal to the element (with a lower flow rate), which take place mainly between protons and electrons.

Such a network, quantified by these numerous particles (atoms, neutrons, protons and electrons) and the links between those particles, is called a *quantum network*.

2.1.2. Quantum network isotopes

An element is the set of atoms that have the same atomic number, Z. The atoms of an element (even Z) that differ in their mass number A are the isotopes of that element. This concept of network isotope could be used to study network variants for optimization purposes.

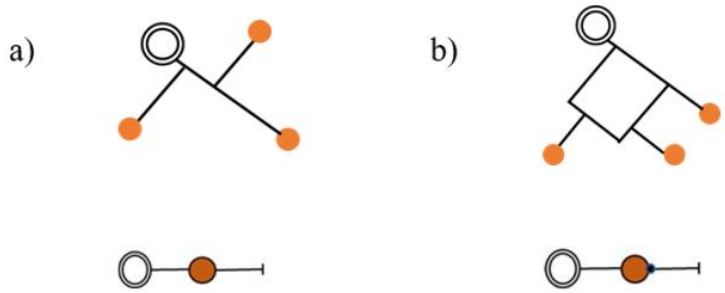

Figure 8: Isotope diagrams; branched structure or meshed structure a) Isotope 3 of element X, 3 protons and 0 neutrons, b) Isotope 4 of element X, 3 protons and 1 neutron

The isotope ${}^{3}_{3}X$ designates the variant of a branched structure (line or pin) with 3 substations, therefore having p = 3 protons (3 electrons) and n = 0 neutrons. The isotope ${}^{4}_{3}X$ designates the meshed variant with p = 4 protons, n = 1 neutron and with a point on the circle of the element to specify the presence of a convergent. This multiple form of representing any network, based either on isotopes of atomic elements X (clusters) or on links of elements made up of protons P (substations), or both, will allow to provide models and perform calculations for complex networks (multi-stage or multisource, meshed or branched).

Quantum network clustering graph: A connection between different atoms and/or isotopes may be performed in a quantum network to create a network of clusters. Figure X illustrates this quantum network clustering graph. In such a graph, only sources, divergents and clusters are represented. Each cluster that is considered as an atom may itself contain divergent and/or convergent, substations, supply tees or any other energy equipment (source or sink). It can thus be defined by its capacity to connect all substations; its efficiency, temperature and pressure levels, as well as the characteristics of the branches and segments that supply energy to substations. The cluster can also contain branched or meshed circuit elements (refer to the examples in Fig. 8). In the latter case, the presence of a Convergent in the loop is represented by a point on the cluster circle. Figure 3 presents an example of a branch-type cluster including Divergents, Tees and Substations.

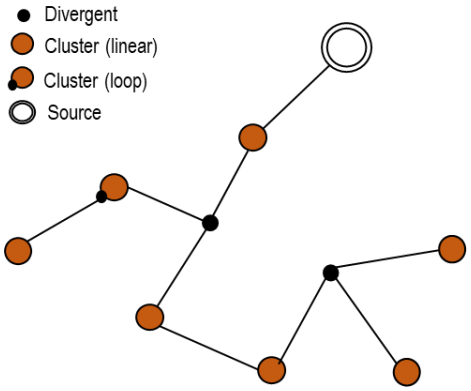

Fig. 2. A cluster-based model in a quantum network with 1 Source, 2 Divergents and 7 Clusters

2.1.3. Network quantum numbers and models

The energy levels that the particles (atoms, neutrons, protons and / or electrons) can reach in the network, as well as their position in the branches or segments (layers or sublayers), are described by 4 parameters or quantum numbers. These quantum numbers are called: primary, secondary, sublayer and flow quantum numbers.

The primary quantum number (n): this number is represented by the number of neutrons in the network (divergents). It takes the value n = 1, 2, 3, 4, ..., and will characterize the number of branches on the network. For a given network, there can only be 2n+1 branches. For example, in the network presented in Figure 7, there are mainly 2 neutrons (n = 2), which correspond to 5 branches.

The secondary quantum number (l): this number defines the particular branches in the primary network. It takes the following values: l = -n,…, -1, 0, +1,…, + n. With a network of n neutrons:

n=0	l = 0	1 branch
n=1	l = -1, 0, +1	3 branches
n=2	l = -2, -1, 0, +1, +2	5 branches
n=3	l = -3, -2, -1, 0, +1, +2, +3	7 branches

The sublayer quantum number (k): this number defines the segments in the branch. It represents the sublayer that is designated by a lowercase letter: s, p, d, f, ... There can be several segments in a branch. The total number of segments in a network is given by the sum of the numbers of neutrons and protons (k = n + p), or by the number of mass (A) defined above.

The flow quantum number (μ): this number is related to the quantity of flow transported by the segment to the proton and/or the neutron. It can take the values μ = -μ, 0, + μ. A particular segment defined by l and k can indeed only lead to a proton and/or a neutron. The quantum state of a segment could then be noted with: $l \cdot k^{\mu}$. Example $-3s^2$ means that the segment s of the branch -3 carries a mass-flow that is twice higher than the average mass-flow that circulates in the network.

Figure 19 shows some examples of networks using the quantum numbers above to specify the location of atoms in different segments. A network pyramid also featured next to each variant. It illustrates the link between the divergent and the branches.

2.2. Quantum network energy models

2.2.1. Quantum flow number modelling and mass-flow balance

The network provides the amount of flow energy necessary for use by substations (electrons). Substations transfer energy from the network to consumers, generally through heat exchangers, or heat pumps for lower temperature networks. As a result, substations generate a temperature difference between the inlet and outlet of the network distribution circuit. To determine network performance, it is necessary to determine the mass flow, in kg/s, conveyed by each branch (layer) and segment (sublayer) of the network.

Based on the hypothesis of a steady state application, the mass flow $\dot{M}_p$ conveyed by a Tee (or proton p) of the network is equal to the mass flow delivered to the corresponding substation (or electron e) $\dot{M}_e$ and the total flow conveyed by the source or central plant $\dot{M}_s$ is equal to the sum of the flows of all the substations (electrons or protons):

$$\dot{M}_s = \sum_{p=1}^{Z} \dot{M}_p = \sum_{e=1}^{Z} \dot{M}_e \qquad (1)$$

Where Z represents the atomic number (number of substations or electrons in the network):

When considering the average flow rate of the network ($\dot{M}_s/Z$) as the flow rate of the source $\dot{M}_s$ in relation to the number Z, the flow rate of each substation can be expressed as a function of the total flow rate of the source using the flow coefficient μ_e, which represents the flow quantum number characteristic of the electron, Eq. (2):

$$\dot{M}_e = \mu_e \frac{\dot{M}_s}{Z} \qquad (2a)$$

This substation mass flow rate $\dot{M}_e$ can also be given in function of the nominal average flow rate of the network ($\dot{M}_0/Z$) by considering the flow quantum number μ_e^0 relative to the design working condition:

$$\dot{M}_e = \mu_e^0 \frac{\dot{M}_0}{Z} \qquad (2b)$$

$\dot{M}_0$ represents the maximum (or nominal) flow rate of the source.

By combining equations 2a and 2b, we can therefore determine the following simple relation (Eq. 4):

$$\mu_e \dot{M}_s = \mu_e^0 \dot{M}_0 \qquad \mu_e^0 \leq \mu_e \qquad (2c)$$

Likewise, the mass flow rate $\dot{M}$ conveyed in any particle or element of the network (atoms, neutrons or protons) is equal to the sum of the mass flow rates of the substations (electrons) bounded to that element. That way, the mass flow balance can easily be performed on all elements of the network by using the following equation:

$$\dot{M} = \left(\sum_{e=1}^{m} \mu_e^0 \right) . \frac{\dot{M}_0}{Z} = \mu \frac{\dot{M}_0}{Z} \qquad (3)$$

Where m represents the number of electrons bonded to the element and μ (represents) the sum of all bounded electrons quantum flow numbers. The corresponding mean value $\bar{\mu}$ (or overall quantum flow number) can also be used as a characteristic of the element:

$$\bar{\mu} = \frac{1}{m} \sum_{e=1}^{m} \mu_e^0 \tag{4}$$

Likewise, the quantity of flow transferred in any branch or segment (or sublayer) of a network can be defined if the position of the branch or segment in the network is known (n, l, k), the overall flow quantum number ($\bar{\mu}$) and the number of electrons bounded to the layer or sublayer (m) are known.

In order to determine the electron quantum flow number μ_e, it is necessary to examine the characteristics of the electron (substation) by considering the two following parameters:

- The energy load (q_e^0) exerted by the electron on the network is defined in this work as the quantity of flow energy provided by the network to the substation ($\dot{Y}_e^-$) as a percentage of the potential or maximum energy available from the source ($\dot{Y}_0^+$). This potential can be defined relatively to a referential temperature level (T_0);
- The relative temperature gradient (δ_e^0) that the electron generates between the inlet and the outlet of the network, which, in this quantum network theory, represents the ratio between the differential temperature of the substation (ΔT_e) and the supply temperature level of the source, given also relatively to the reference temperature ($T_s^0 = T_s - T_0$).

Considering these definitions above, the load of energy can be expressed with the following equation:

$$q_e^0 = \frac{\dot{Y}_e^-}{\dot{Y}_0^+} = \frac{\dot{M}_e}{\dot{M}_0} \cdot \frac{\Delta T_e}{T_s - T_0} \tag{4a}$$

Or then:

$$q_e^0 = \frac{\dot{Y}_e^-}{\dot{Y}_0^+} = \frac{\dot{M}_e}{\dot{M}_0} \cdot \delta_e^0 \tag{4b}$$

This factor $\delta_e^0 = \Delta T_e / T_s^0$ is an important dimensionless parameter that can be used to characterize the performance of the substation. The corresponding mean value ($\bar{\delta}_e^0$) given by the following relation (Eq. 5) is, in practice, a good indicator to estimate the working performance of the global network:

$$\bar{\delta}_e^0 = \frac{1}{Z} \sum_{e=1}^{Z} \delta_e^0 \tag{5}$$

For a reference temperature equal to $T_0 = 0°C$, the values of δ_e^0 are generally between 1/10 and 2/3. Generally, a low value of δ_e^0 corresponds to a low-grade or anergic type network or also to the very low performance of a high temperature (HT) network system. A high value of δ_e^0 corresponds in general to a HT network operating in very good conditions. Figure 9 shows the delta value for different existing networks.

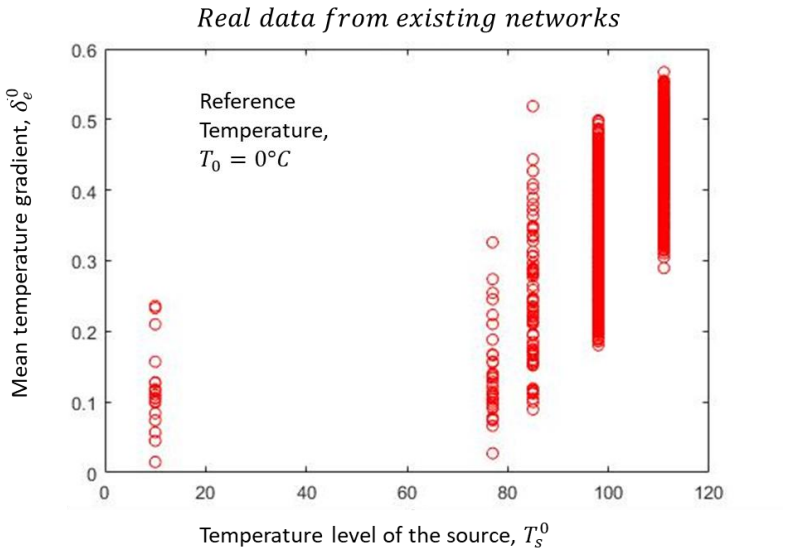

Figure 9: Example of delta in different existing network in Switzerland

By combining equations 2a and 4b, the following relation (Eq. 6) can show that the flow quantum number of the electron is proportional to its load and inversely proportional to the specific differential temperature:

$$\mu_e^0 = Z \cdot \left(\frac{q_e^0}{\delta_e^0} \right) \tag{6}$$

This equation shows that, for the same energy load, low temperature network substations convey more flow and therefore cause more pressure losses in the network.

Substation can also be a source of energy. For example, in thermal smart grids, other decentralized plants (or distributed supply energy units) can be installed in the network. Thus, substations can be consumers (sinks) and/or producers (sources) depending on the conditions (for example, a building using both heat exchangers for heating purposes and solar thermal collectors to supply solar energy to the network). Thus, a substation that withdraws energy from the network is an energy sink substation and its load is counted positively in the network's total energy. A substation that supplies energy to the network is an energy source substation, hence its load will be counted negatively.

2.2.2. Temperature distribution modelling in a quantum network

Let us first examine the temperature variation a fluid flowing in an insulated pipe (Figure 10). T_i represents the initial temperature at the inlet of the pipe and T_f the final temperature at the outlet of the pipe. In practice, if the overall temperature of the fluid inside the pipe is higher than the ambient temperature T_a, the flow occurs with temperature drops, so that the temperature decreases.

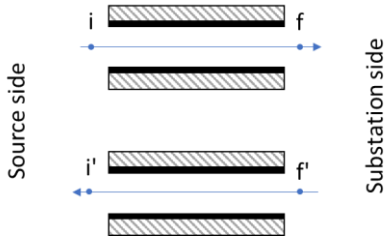

Figure 10: Scheme of the pipe with the nomenclature

By considering a steady state one-dimensional flow hypothesis and the balance of energy exchanged between the fluid and its environment, the following equation is obtained:

$$\frac{T_f^0}{T_i^0} = \frac{T_f - T_a}{T_i - T_a} = \ e^{-\tau} \tag{7}$$

Where τ is a thermal-hydraulic dimensionless factor of the pipe, as shown in equation 8:

$$\tau \ = \frac{U\ L\ D\ \pi}{\dot{M} c_p} \tag{8}$$

With U the overall heat transfer coefficient of the pipe, L the length, D the internal diameter, $\dot{M}$ the mass flow rate carried in the pipe and c_p the specific heat per unit of mass. The overall heat transfer coefficient of an underground pipe with insulation (Figure 11) can be determined by equation 9

$$U = \frac{1}{\frac{1}{h_i} + \frac{r_1 \cdot ln(r_3/r_2)}{\lambda_{in}} + \frac{r_1 \cdot ln(r_2/r_1)}{\lambda_{steel}}} \quad (9)$$

where h_i is the heat transfer coefficient determined by the Gnielinski correlation [22], λ (is) the thermal conductivity of the pipe and the insulation, r_1 (is) the inner radius of the pipe, r_2 (is) the radius at the intersection of metal and insulation and r_3 (is) the outer radius of the insulation.

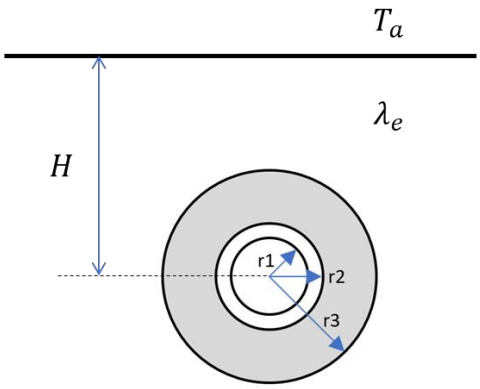

Figure 11: Section of a pipe with insulation

Let us now consider the variation of temperature of a media in a segment (or sublayer) of a network represented. The sublayer is composed of thermal network pipes, typically arranged in pairs (supply and return pipes), which are supposed to have the same characteristic in terms of τ (i.e., same diameter, length, overall heat transfer coefficient and mass flow rate).

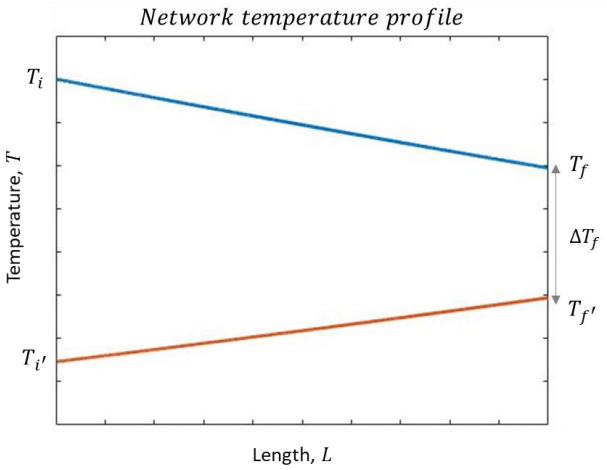

Figure 12: Example of temperature profile of the media in function of the length in the pipe

In addition to temperatures losses on the supply and return pipes, a temperature difference is generated on all substations that are supplied through this segment. Like the definition given in equation 5, $\delta = \Delta T_f / T_f^0$ represents the relative temperature difference occurring at the consumer side of the segment:

$$\delta = \Delta T_f / T_f^0 = \frac{\Delta T_f}{T_f - T_a} \tag{10}$$

By considering equation 10 and applying expression 7 for temperature losses to the supply and return pipes, the following expressions can be determined:

$$\frac{T_f^0}{T_i^0} = e^{-\tau} \qquad \frac{T_{i'}^0}{T_f^0} = e^{-\tau} \tag{11}$$

$$\frac{T_{f'}^0}{T_f^0} = 1 - \delta \tag{12}$$

From these equations, one can deduce and express a simple relation giving the ratio of temperature levels of the fluid between the return and supply pipes in function of the dimensionless parameters (τ, δ) that are characteristics of the segment:

$$\frac{T_{i'}^0}{T_i^0} = e^{-2\tau}(1 - \delta) \tag{13}$$

Equation 13 can be used to determine the distribution of temperature in all segments of the network when first knowing the departure temperature from the plant and the differential temperature occurring on each substation.

2.2.3. Pressure drop distribution in quantum network

Linear pressure losses ΔP_l are calculated as follows with equation 7,

$$\Delta P_l = \rho \cdot f \cdot \frac{L}{d} \cdot \frac{\mathrm{v}^2}{2} \quad (1)$$

where ρ is the density of the fluid, f (is) the friction factor determined with the Goudar–Sonnad equation [23] as function of the pipe's roughness; and Reynold's number, L is the length of the pipe, d (is) the diameter of the pipe and v (is) the fluid velocity inside the pipe. Singular pressure losses (exchangers, valves, elbows, tees) are assessed with conventional models.

2.2.4. Quantum network energy formulation and modelling

As previously seen, the flow between the source and the substations in the quantum network is quantified according to the flow quantum number equation (Eq. 3), and the distribution of temperature in the network's branches and segments is determined in function of dimensionless parameters (Eq.13). Thus, the distribution of flow energy in the network's branches and segments could be modelled and simulated by using all these parameters and quantum numbers.

The first law of thermodynamics (or energy balance equation) applied to the segment in steady-state operation makes it possible to express the heat transfer energy loss ($\dot{Q}^-$) in function of the flow energy received by the segment from the source ($\dot{Y}^+$) and the effectiveness of the transmission process (ε):

$$\dot{Q}_a = (1 - \varepsilon)\, \dot{Y}^+ \quad (14)$$

Where $\varepsilon = \dot{Y}^- / \dot{Y}^+$ represents the ratio between the flow-energy provided by the segment ($\dot{Y}^-$) and the flow-energy received from the source ($\dot{Y}^+$).

In this quantum network modelling, the minimum value of $\dot{Y}^+$ represents the energy level that the system (or sublayer) can reach in the network and is called quantum network energy. The corresponding value of ε is the quantum network effectiveness.

Quantum network energy

Let us model the flow energy $\dot{Y}^+$ by considering a HTF with a constant specific heat per unit of mass. For a real fluid application with no phase-change, the specific heat mean-value is used, defined as the ratio between the differential enthalpy and the corresponding differential temperature in the same condition ($\bar{c}_p = \Delta h/\Delta T$). $\dot{Y}^+$could then be expressed by the following:

$$\dot{Y}^+ = \dot{M}\ \bar{c}_p\ (T_i - T_{i'}) = \ \dot{M}\ \ \bar{c}_p\ [\ (T_i - T_a) - \ (T_{i'} - T_a)\ ] \tag{15}$$

Or then:

$$\dot{Y}^+ = \dot{M}\ \bar{c}_p\ (T_i - T_a)\ \ \left[\ 1 - \frac{T_{i'} - T_a}{T_i - T_a}\right] \tag{16}$$

From the development given in sections 2.2.1 and 2.2.2 (Eq. 3 and Eq. 13), the following equations can thus be developed:

$$\dot{Y}^+ = \mu\ \frac{\dot{M}_0}{Z}\ \bar{c}_p\ T_i^0 \left[\ 1\ -\ \frac{T_{i'}^0}{T_i^0}\right] \tag{17}$$

$$\dot{Y}^+ = m\,.\left(\frac{\dot{M}_0}{Z}\ \bar{c}_p\right).\ \bar{\mu}\ \ [\ 1 - e^{-2\tau}(1-\delta)\ ]\ T_i^0 \tag{18}$$

Thus, the distribution of flow energy in the network's branches and segments could finally be expressed by using quanta (distribution of energy on the basis of discontinuous quantities):

$$\dot{Y}^+ = m\ k_0\ \bar{\nu} \qquad or \qquad \dot{y}^+ = \ \dot{Y}^+/m = k_0\ \bar{\nu} \tag{19}$$

The quantum network energy ($\dot{y}^+$) is the minimum quantity of flow-energy to be transferred in a branch or segment of a network and is given as a constant multiple (k_0) of a simple "quantum state function" ($\bar{\nu}$), the letter being characteristic of the layer or sublayer:

$$\bar{\nu} = \bar{\mu}\ \ [\ 1 - e^{-2\tau}(1-\delta)]\ T_i^0 \qquad\qquad k_0 = \dot{M}_0 c_p/Z \tag{20}$$

The coefficient k_0 of the network or "Kane's factor" is a key characteristic parameter of the size and density of the network. It could be used to classify different networks according to their production capacity and to the number of connected substations.

The quantum state function $\bar{\nu}$ depends on the flow quantum number ($\bar{\mu}$) and the dimensionless characteristic parameters of the layer or sublayer (τ, δ), and is a function of the temperature level of the fluid (T_i^0). This state function is not really proportional to the temperature level of the fluid. To illustrate this, let us determine the expression showing the relationship between the quantum state function $\bar{\nu}$ and the effectiveness of the process ε.

Quantum network effectiveness

By considering the same development above, the flow-energy service provided by the branch or segment of the network can be determined by the following relation:

$$\dot{Y}^- = m\,.\left(\frac{\dot{M}_0}{Z}\,\bar{c}_p\right).\bar{\mu}\;\;\delta\,T_f^0 \tag{21}$$

Given Eq. 18 and Eq. 20, the effectiveness of the heat transfer process in a segment can be expressed by the following relationships:

$$\varepsilon = \dot{Y}^-/\dot{Y}^+ = \frac{\delta}{1-e^{-2\tau}(1-\delta)}\;\frac{T_f^0}{T_i^0} \tag{22}$$

$$\varepsilon = \dot{Y}^-/\dot{Y}^+ = \frac{\bar{\mu}\,\delta}{\bar{\nu}}\;T_f^0 \tag{23}$$

From equations Eq. 11 and Eq. 22, effectiveness can be explicitly expressed as a function of the thermo-hydraulic dimensionless factor (τ) and the relative differential temperature (δ), both are used as characteristics of the layer or sublayer:

$$\varepsilon = \frac{\delta\;e^{-\tau}}{1-e^{-2\tau}(1-\delta)} \tag{24}$$

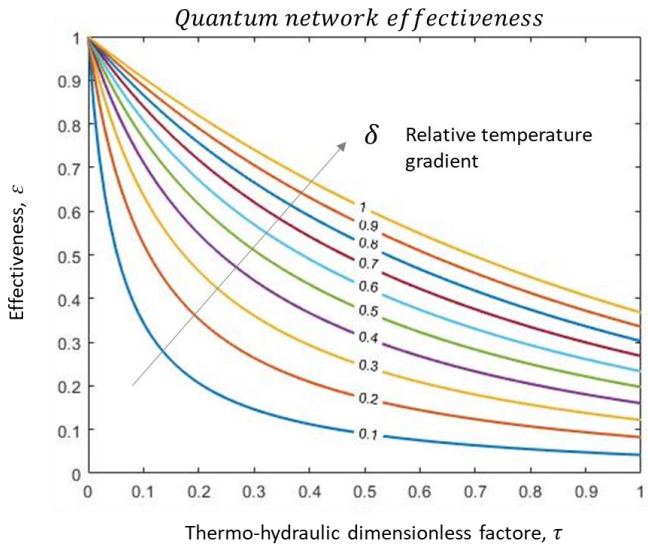

Figure 13: Effectiveness in function of the dimensionless factors

Figure 13 shows the effect of these parameters on effectiveness. Effectiveness is equal to one (epsilon=1) for a dimensionless factor equal to zero ($\tau = 0$) and decreases exponentially for higher values of τ. For the same value of τ, the performance of the process is better for systems at higher differential temperature (δ). That is why, for the same pipe characteristics (e.g. diameter, length and global heat transfer coefficient), the effectiveness of an urban network system is greater in winter for heating at higher differential temperature (δ) and lower dimensionless factor (τ, corresponding to high mass flow rate) than in summer for hot water production only. It is in our best interest to achieve an adiabat process with no atmospheric losses ($\varepsilon \cong 1$), with a high temperature difference but also with a low dimensionless factor ($\tau \cong 0$).

From equations Eq. 11 and Eq. 23, a general relationship can be deduced for effectiveness, as a function of the quantum state function, the dimensionless parameters used to characterize the layer of sublayer and the temperature level of the fluid:

$$\varepsilon = \frac{\bar{\mu}\,\delta}{\bar{\nu}} T_f^0 \qquad or \qquad \varepsilon = \frac{\bar{\mu}\,\delta}{\bar{\nu}} T_i^0\, e^{-\tau} \tag{25}$$

Or then:

$$\varepsilon = \frac{\bar{\mu}\,\Delta T_f}{\bar{\nu}} \tag{26}$$

These relationships (Eq. 25 and Eq. 26) clearly express the link between effectiveness and all the parameters that characterize the system's performance. For the same differential temperature at the outlet of the segment, effectiveness is higher the lower the quantum state function (is). The quantum state function plays an important role in the optimization of the flow-energy distribution.

2.2.5. Cluster energy modelling

Such a quantum network energy formulation has several advantages:

1- Different branches (or layers) of the network supplying energy to different substations can then be simulated and computed separately in parallel, without any iteration procedures if the layer quantum state function $\bar{\nu}_{ls}$ is known in function of the quantum numbers ($l \cdot s^{\mu}$) and the dimensionless characteristic parameters (τ, δ):

$$\bar{\nu}_{ls} = \left[\frac{\bar{\mu}\,\delta}{\varepsilon} T_i^0\, e^{-\tau} \right]_{ls} \tag{27}$$

2- Any group of substations receiving energy from a segment (or sublayer k) of the network can be considered as a cluster or atom with the symbol of ${}^{A_k}_{Z_k}X_k$, for which its state of energy is entirely determined with the knowledge of the sublayer quantum state function $\bar{\nu}_{lk}$ in function of the quantum numbers ($l \cdot k^{\mu}$) and the dimensionless characteristic parameters (τ, δ):

$$\bar{\nu}_{lk} = \left[\frac{\bar{\mu}\,\delta}{\varepsilon} T_i^0\, e^{-\tau} \right]_{lk} \tag{28}$$

3- In addition to the energy modeling of layers and sublayers, the quantum state function formula (Eq. 20 and Eq. 25) can be used to model and simulate the energy level of any component (or particle) in the network. The $\bar{\nu}$ values of some components or particles are given by the following:

Substation (Electron, m=1, $\bar{\mu} = \mu_e$): $\bar{\nu}_e = \mu_e \delta_e T_e^0$

Tee (Proton ${}^1_1P$, m=1, $\bar{\mu} = \mu_p = \mu_e$): $\bar{\nu}_p = \mu_p \delta_p T_p^0 = \frac{\mu_e\,\delta_e}{\varepsilon} T_e^0\, e^{-\tau_e}$

Divergent (Neutron, $\bar{\mu} = \bar{\mu}_n$): $\bar{\nu}_n = \bar{\mu}_n \delta_n T_n^0 = \left[\frac{\bar{\mu}\,\delta}{\varepsilon} T_i^0\, e^{-\tau} \right]_{l,k}$

Central plant (Atom ${}^A_Z X$, m=Z, $\bar{\mu} = \bar{\mu}_0 = 1$): $\bar{\nu}_n = \mu_0 \delta_0 T_s^0 = \left[\frac{\bar{\mu}\,\delta}{\varepsilon} T_s^0\, e^{-\tau} \right]_{0s}$

4- The same formulation can be used in a detailed design phase or an operating network, if all design and operational parameters are known (e.g., diameter, length and global heat transfer coefficient); or globally, through an optimization process in a conceptual design phase so as to know the optimal dimensionless parameters.

3. Application of the quantum network methodology and validation

3.1. Converting an existing DHC network in a quantum network

Figure 14 shows an existing district heating/cooling network (DHC) that operates through a system

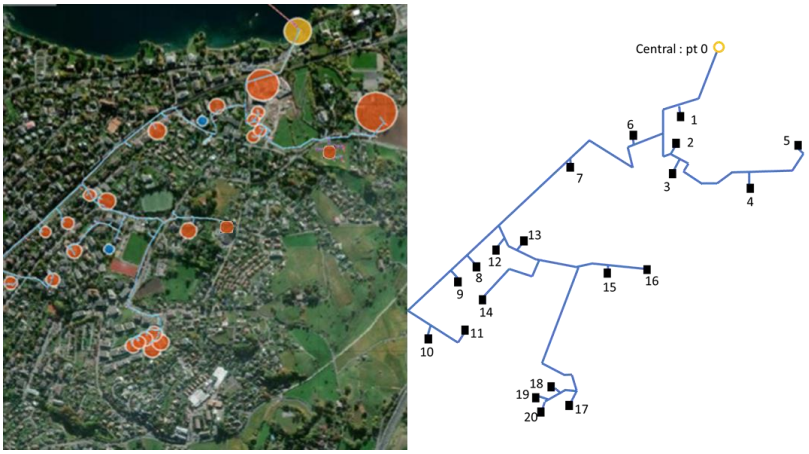

Figure 14: Example of a real network to a quantum network. The plant is the station of the heat pumps in the lake. The network distribution links the plant to a living neighborhood

combining a lake water pumping station, an anergy glycol water network and decentralized heat pumps in the substations. The water, collected at a depth of around 70 meters, will transfer its energy to the DHC anergy network at temperature levels between 7 and 10°C and via a heat exchanger. When it returns to the lake, it has lost 3°C, at pumping station level. The decentralized heat pumps are used to recover energy from the network and to supply heat to buildings at higher temperature levels (between 35°C and 65°C). Each building can then be supplied with heating and DHW by means of this water.

The conversion from this real existing network to a corresponding quantum network can be done in a simple way and in different steps:

Identifying the atomic element symbolizing the network ($^{A}_{Z}X$):

The initial objective for the study of such a network is to first determine the atomic number Z and the mass number A characterizing the network. To do this, the simplified diagram is used in Figure 15 to identify and number the different particles, namely neutrons (divergent), protons (tees) and electrons (substations). The total number of neutrons corresponds to the principal quantum number n=3; and the total number of electrons or protons p=20 corresponds to the atomic number Z=20. The sum of these two quantities gives the mass number, also representing the number of network segments (A=n+p=23). The atomic element corresponding to Figure 15 is thus defined by the symbol ($^{23}_{20}X$)

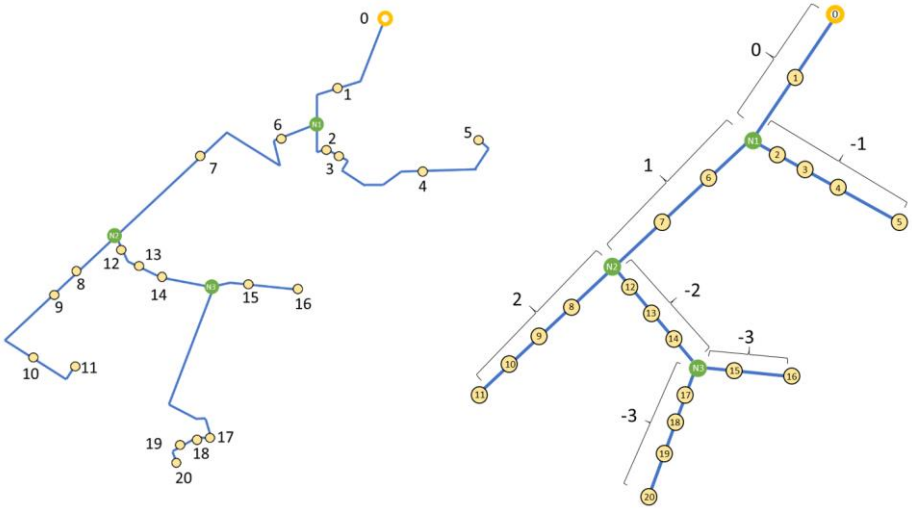

Figure 15 : Simple diagram of the real network with a view to creating a quantum network

Characterizing and specifying electrons in the quantum network:

The substations or electrons energy data analysis (power, flow and/or temperature difference), based on the development given in section 2.2.1, makes it possible to determine the energy load (q_e^0), the specific differential temperature (δ_e^0) and/or the value of the quantum flow number (μ_e) of each electron in the network. The electron's specification makes it possible to list these different input parameters necessary for the simulation (Table 1).

Table 1 : Table of quantum network position with the position of particles for the network with heat pumps

Substation	Heat rate [kW]	ΔT [°C]	Flow [kg/s]	q_e^0	δ_e^0	μ_e^0
1	342.8	2.13	38.38	0.0448	0.2134	4.20
2	17.9	1.52	2.82	0.0023	0.1517	0.31
3	18.8	1.52	2.95	0.0024	0.1519	0.32
4	11.0	1.50	1.75	0.0014	0.1504	0.19
5	535.6	2.50	51.18	0.0699	0.2500	5.59
6	47.0	1.57	7.14	0.0061	0.1572	0.78
7	74.2	1.62	10.92	0.0097	0.1624	1.19
8	25.7	1.53	4.00	0.0033	0.1532	0.44
9	8.8	1.50	1.41	0.0012	0.1500	0.15
10	28.2	1.54	4.38	0.0037	0.1537	0.48
11	9.2	1.50	1.47	0.0012	0.1501	0.16
12	15.7	1.51	2.48	0.0021	0.1513	0.27
13	73.9	1.62	10.88	0.0097	0.1624	1.19
14	40.3	1.56	6.18	0.0053	0.1560	0.68
15	56.5	1.59	8.49	0.0074	0.1590	0.93
16	54.3	1.59	8.18	0.0071	0.1586	0.89
17	43.4	1.57	6.62	0.0057	0.1566	0.72
18	32.2	1.54	4.99	0.0042	0.1544	0.55
19	20.5	1.52	3.22	0.0027	0.1522	0.35
20	36.0	1.55	5.54	0.0047	0.1552	0.61

Establishing the table of quantum numbers:

*Table 2: Table **of quantum numbers** for the network with heat pumps*

l		**-3**	**-2**	-1	0	1	**2**	**3**
k	s	15	12	2	1	6	8	17
	p	16	13	3	-	7	9	18
	d		14	4		-	10	19
	f		-	5			11	20
n			**3**		1	**2**		

μ_l^0		1.82	6.18	6.42	20.00	9.39	1.23	2.23
μ_e^0	s	0.93	0.27	0.31	4.20	0.78	0.44	0.72
	p	0.89	1.19	0.32	-	1.19	0.15	0.55
	d		0.68	0.19		-	0.48	0.35
	f		-	5.59			0.16	0.61
μ_n^0			4.05		15.80	7.41		

With the quantum number n=3, one can calculate the number of branches (2n+1=7) and segments (A=23) of the network and thus determine the quantum numbers (l, k, μ) locating each electron of the network. Such an analysis leads to the establishment of a simple table of quantum numbers given in (Table 2). In this table, the secondary quantum number l determines the 7 branches of the network, the principal quantum number n identifies the position of each of the 3 neutrons on the branches and the parameter k (s, p, d, f) locates the substations in segments. The table is filled with the quantum flow number μ_e for electrons (yellow part) and $\mu_n$for neutrons (green part).

The sum of μ in each column in this table makes it possible to determine the flow quantum number (μ_l) in the corresponding branch. The flow carried through the branch is determined according to Eq.3.

Simulating and analyzing quantum parameters:

Once the values are included in the table, the network can be simulated and the network's quantum numbers are computed for the nominal heat rate and/or for the entire year.

Figures 16 and 17 respectively show the main results () of the simulation for the main layer (0s) and at each hour over the year, as well as the quantum numbers for each branch or layer. It can be shown that the flow-energy is relatively low in summer corresponding to the low mass flow rate ($\dot{M}_0$). Effectiveness is lower and the quantum state function is higher. During the winter, the effectiveness is relatively high above 95%.

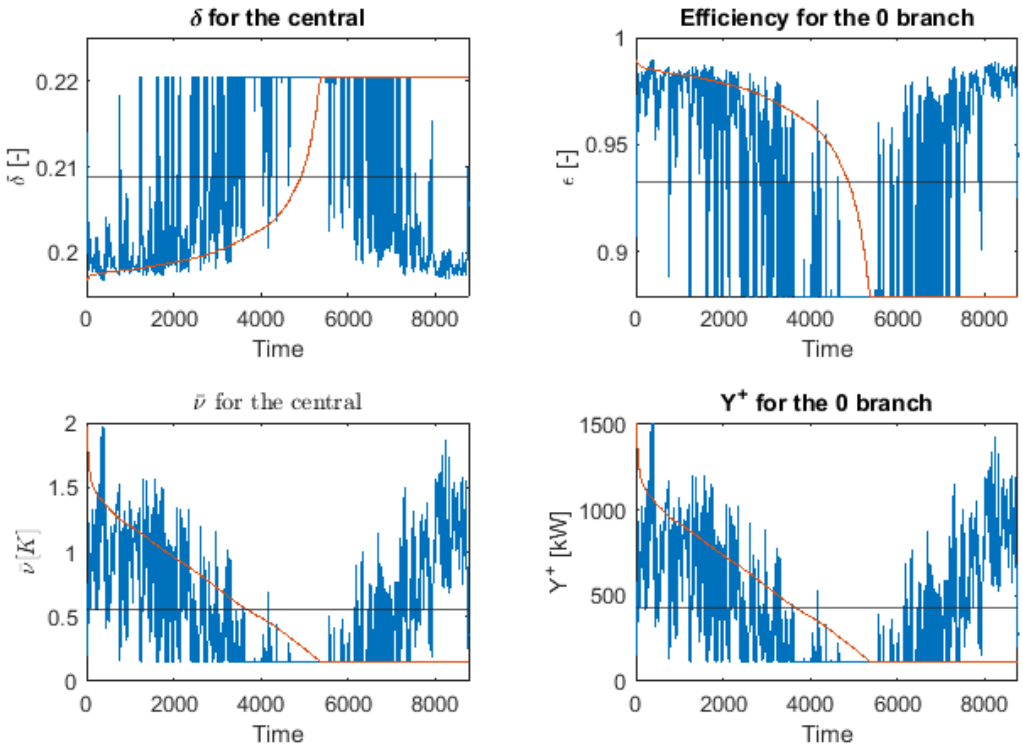

Figure 16: Per hour quantum numbers over the year for a network with heat pumps

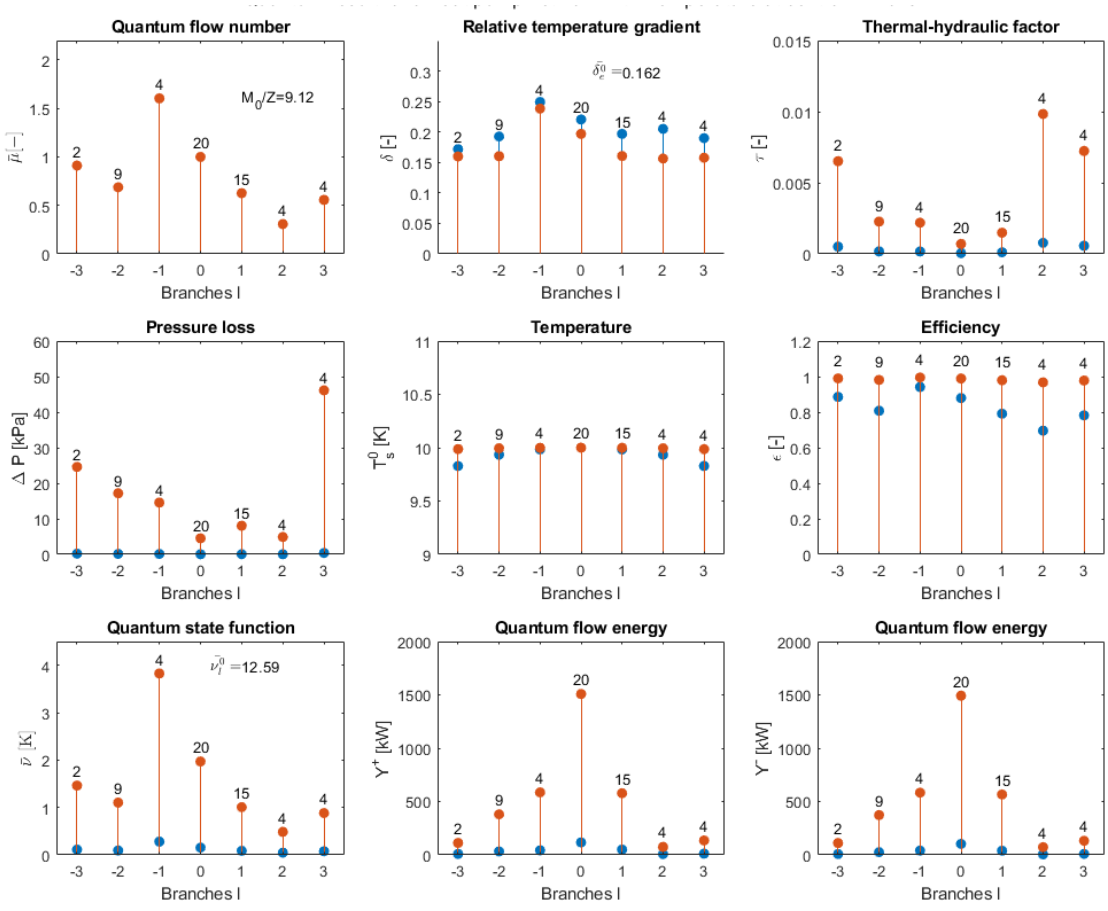

Figure 17: Quantum numbers for each branch with the nominal (blue), mean (black) and extreme (red) values

For this type of low-temperature DHC anergy network, factor δ in any branch (segment s of the branch) remains very small over the year. Nominal effectiveness is very close to unity / 1 (100%), corresponding to a thermal-hydraulic dimensionless factor value almost close to zero (heat losses are low for an anergy network at low temperature).

The quantum state function ($\bar{\nu}$) follows the same evolution as the flow quantum number ($\bar{\mu}$). The latter provides information about the largest energy consumers (or substations). It can be noted, for example, that branch or layer -1 conveys a throughput twice as high as the average value defined by Mo/Z for the network. It also supplies energy to only 4 out of the 20 complete substations of this network.

Example of clustering: grouping a number of substations in the network to form a cluster

A part of this existing DHC network could be considered as a cluster and therefore transformed as an atom into the quantum network. Figure 18 shows an example of a cluster or atom ($^{15}_{13}X$) in the quantum network (the number of electrons/protons is known as p=13 as well as the number of neutrons as n=2). In this case, the computational time of the quantum network is reduced without any loss of information because the state of energy of the atom ($\dot{Y}^{-}_{1d}$) is entirely determined with the knowledge of the 1d-sublayer (Eq. 21): quantum state function corresponding to 1d-sublayer $\bar{\nu}_{1d}$:

$$\dot{Y}^{-}_{1d} = \left[m \,.\left(\frac{\dot{M}_0}{Z}\,\bar{c}_p\right).\bar{\mu}\;\delta\,T_f^0\right]_{1d} \qquad m = 13, \qquad Z = 20 \qquad (21)$$

The calculation considers the total number of electrons in the quantum network (Z=20) and the number of electrons in the atom (m=13). The quantum numbers for the others particles remain unchanged compared with the previous configuration. Tables 3 and 4 respectively give the input parameters and quantum numbers.

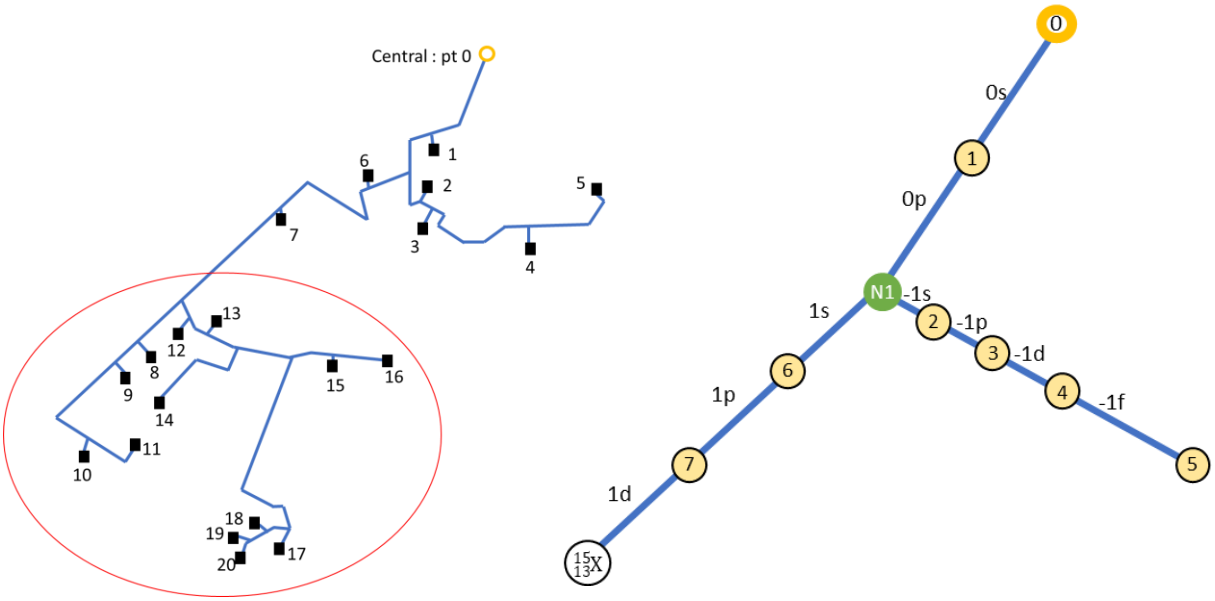

Figure 18: Example of a network with cluster

Table 3: Table of quantum network position with the position of particles for the network with heat pumps with an atom

Substation	Heat rate [kW]	ΔT [°C]	Flow [kg/s]	q_e^0	δ_e^0	μ_e^0
1	342.8	2.13	38.38	0.0509	0.213	4.77
2	17.9	1.52	2.82	0.0027	0.152	0.35
3	18.8	1.52	2.95	0.0028	0.152	0.37
4	11.0	1.50	1.75	0.0016	0.150	0.22
5	535.6	2.50	51.18	0.0796	0.250	6.37
6	47.0	1.57	7.14	0.0070	0.157	0.89
7	74.2	1.62	10.92	0.0110	0.162	1.36
$^{15}_{13}X$	444.8	2.33	45.65	0.0661	0.233	5.68

Table 4: Table of quantum numbers for the reduced network

μ_l^0		7.30	20.00	7.93
μ_e^0	s	0.35	4.77	0.89
	p	0.37	-	1.36
	d	0.22		5.68
	f	6.37		
μ_n^0			15.23	

3.2. Optimization with a variety of network configurations (isotopes)

The path in the network impacts energy losses and therefore energy distribution, too. A simple optimization can be done by comparing different network configurations with the same consumers (same electron's specification in the quantum network). Figure 19 shows for example different network configurations for a number of 8 electrons.

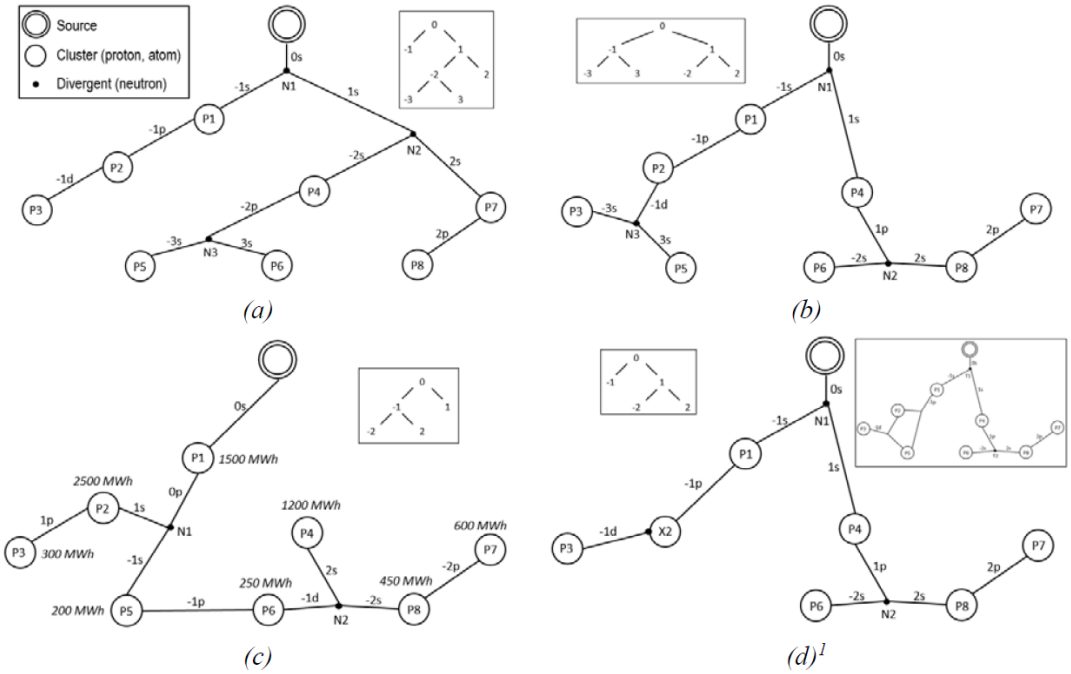

Figure 19: Four versions of 8 substations: a) 8 protons, 3 neutrons, b) 8 protons, 3 neutrons, c) 8 protons, 2 neutrons, d) 6 protons, one 2-proton atom (loop), 2 neutrons

These 4 configurations can be analyzed based on the development given in section 2.1.2:

a) The first configuration corresponds to a branched quantum network of 8 protons and 3 neutrons ($^{11}_{8}X$), with a total length of 2190 m;

b) The second configuration is represented by the same atomic element but with a total length of 1750 m, considering the different path used to provide energy to substations;

c) The third configuration corresponds to isotope-10 of the same element ($^{10}_{8}X$) having to 2 neutrons instead of 3.

d) The last configuration corresponds to isotope-12 of the same element ($^{12}_{8}X$) having a loop in segment -1p. One can distinguish the presence of X2 having a point on the circle of the element to specify the presence of a convergent, as described in section 2.1.2.

Table 5 and table 6 respectively show the specification of electrons and the quantum members of its configuration.

Table 5: Table of quantum numbers for the substations according to the different variants

	Energy	Max power	ΔT	M	q^0	δ^0	μ
	kWh	kW	°C	kg/s	-	-	-
1	1,500,000	621	15	10.40	0.045	0.214	1.685
2	2,500,000	1,035	15	17.34	0.075	0.214	2.809
3	300,000	124	15	2.29	0.010	0.214	0.371
4	1,200,000	497	15	8.32	0.036	0.214	1.348
5	200,000	83	15	1.53	0.007	0.214	0.247
6	250,000	104	15	1.91	0.008	0.214	0.309
7	600,000	249	15	4.16	0.018	0.214	0.674
8	450,000	186	15	3.43	0.015	0.214	0.556

Table 6: Table of quantum network position with particles position according to the different variants

	-3	**-2**	**-1**	**0**	**1**	**2**	**3**

(a)

	0	3	0	1	2	0	0
s	5	4	1			7	6
p			2			8	
d			3				

(b)

	0	0	3	1	2	0	0
s	3	6	1		4	8	5
p			2			7	

(c)

	0	2	1	0	0
s	8	5	1	2	4
p	7	6		3	

(d)

	0	0	1	2	0
s	6	1		4	5
p		X2			7
d		3			

The flow-energy distribution is computed for each segment of the network by considering one year of operation with a one-hour time step. Thanks to that, the heat and pressure losses are known for each segment.

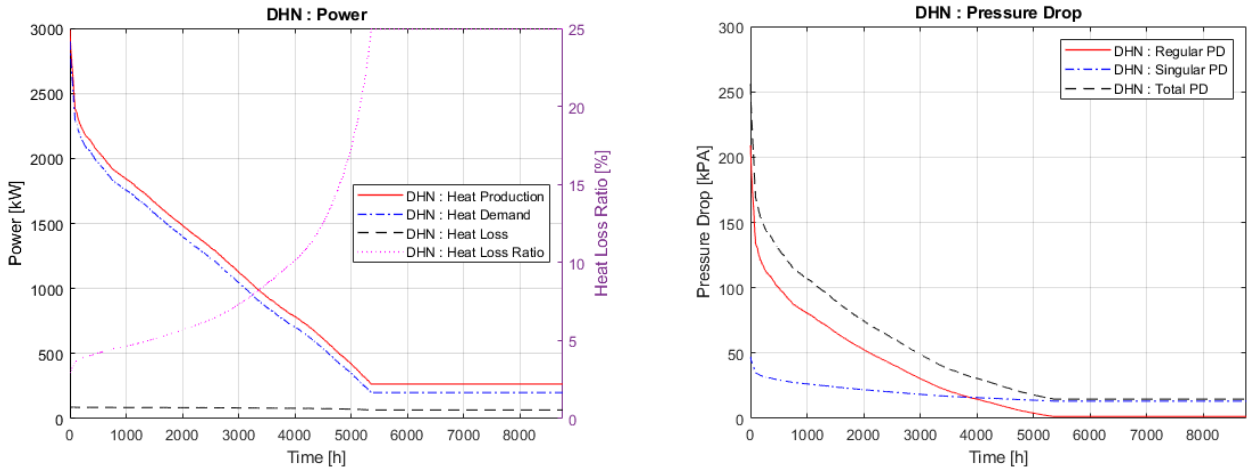

Figure 20: Characteristics of the (a) variant: a) DHN power, b) DHN pressure drops

Figure 20 shows for configuration (a) and respectively the cumulated power curves and pressure drop in the network over the year. The nominal heat rate supplied by the source to the DHN is in the order of 2887 kW, with an annual energy production of around 7'658 MWh/y. The heat losses vary from 2.4% to 22.2% of the power supplied during the year. A maximum 256-kPa pressure loss is obtained, corresponding to around 117 Pa/m. The summer period (~5500-8760h), during which only domestic hot water production is required, is clearly visible. Table 7 summarizes the main results obtained for all network configurations (figure 19).

Table 7: Comparison of four DH networks

Variant	(a)	(b)	(c)	(d)
Network supply length, m	2190	1750	1830	1610*
Nominal mass flow rate, kg/s	46.12	46.12	46.12	46.12
$\frac{\dot{M}_0}{Z}$	5.77	5.77	5.77	5.77
Heat demand, MWh/y	7000	7000	7000	7000
Nominal power, kW	2987	2971	2983	2972
Heat loss, MWh/y	663	546	637	564
Heat loss ratio, %	8.658	7.240	8.347	7.451
Nominal pressure drops, bar	2.56	3.08	3.12	2.64

**Reduced network*

Variant (a) exhibits more thermal losses because of the longer network length (2190m). However, the nominal pressure drop is lower compared to other configurations, thanks to the right repartition of the substation in the network. Variant (b) represents the optimal solution in term of heat losses, though the pressure drop is higher, in the order of 308 kPa (176 Pa/m). Variant (c), which uses only 2 neutrons, carries higher flow rates throughout the network compared to others variants. Thermal and pressure losses are more significant. Variant (d) seems a more balanced network and represents the relatively optimal solution in term of pressure and thermal losses. Figure 20 compares the quantum state functions in each branch and for the different variants. It shows the energy distribution in all branches and also gives an indication about the location of substations with higher energy density.

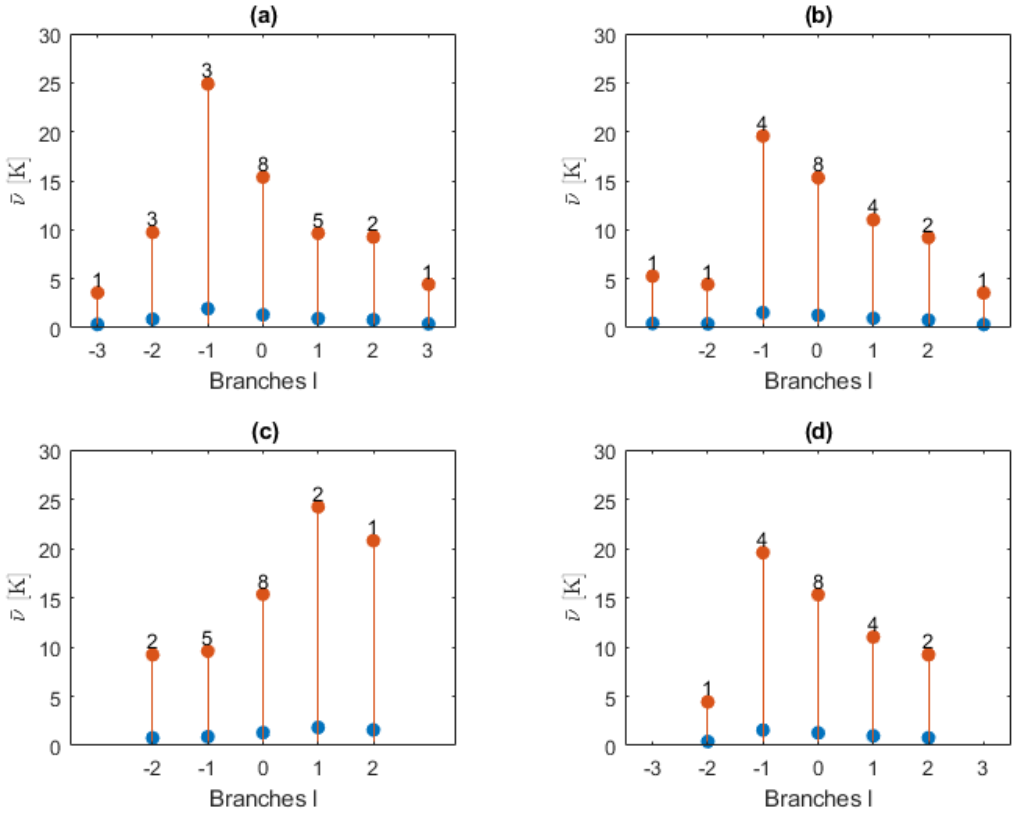

Figure 21: Quantum state functions for each branch with the maximum (red) and minimum (blue) values

3.3. Comparison with simulated data from Neplan

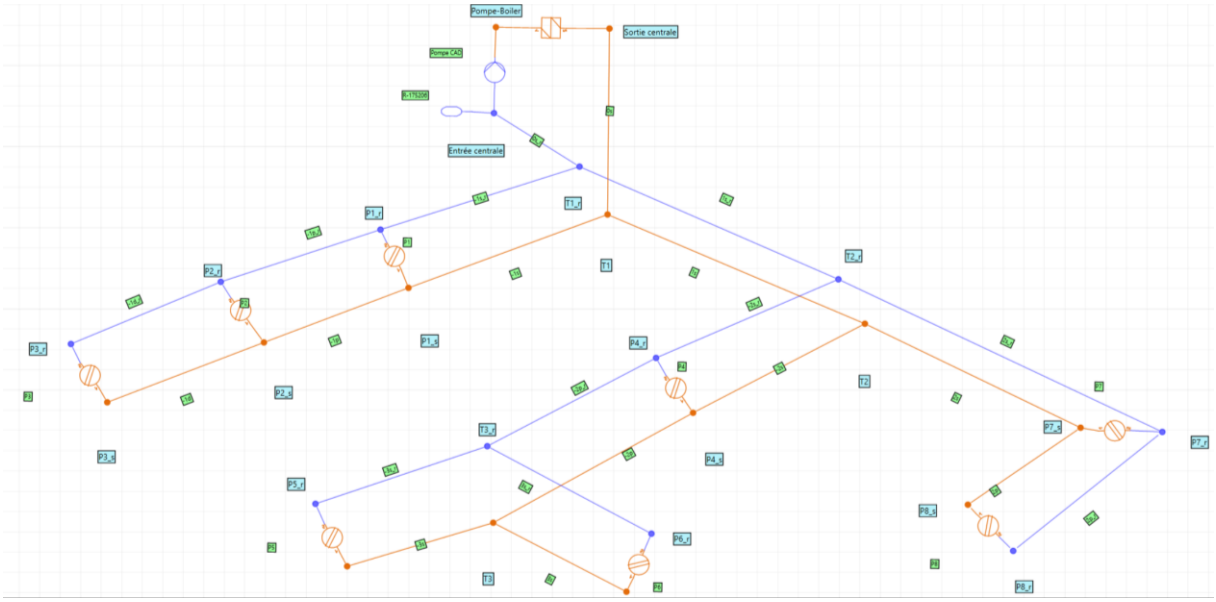

Figure 22: NEPLAN network visualisation of the network on NEPLAN

Table 8: Using properties for variant (a) for NEPLAN

	-3	-2		-1			0	1	2		3
	s	s	p	s	p	d	s	s	s	p	s
Length [m]	150	240	250	190	220	210	60	300	230	190	150
Diameter [mm]	54.5	107.1	70.3	160.3	132.5	54.5	210.1	132.5	107	70.3	54.5
U [W/m2K]	0.19	0.25	0.22	0.34	0.29	0.20	0.36	0.29	0.24	0.22	0.19

In order to validate the models developed for flow, pressure and temperature distributions in the network, a comparison with the NEPLAN simulation software has been performed, based on variant (a) at nominal load. A 70°C network supply temperature and a 15°C temperature difference in the substations are taken into consideration. Table 9 shows the results for each segment of the network.

Table 9 : Comparison of the conventional value

		-3	-2		-1			0	1	2		3
		s	s	p	s	p	d	s	s	s	p	s
Quantum N.	Flow [kg/s]	1.32	10.87	2.97	28.33	18.45	1.98	46.12	17.79	6.92	2.97	1.65
	Pressure drop [bar]	0.101	0.299	0.218	0.194	0.258	0.306	0.040	0.328	0.121	0.166	0.154
	T inlet [°C]	69.37	69.88	69.77	69.99	69.94	69.86	70.00	69.99	69.88	69.71	69.37
	T return [°C]	53.57	54.29	53.35	54.76	54.72	54.10	54.55	54.23	54.35	54.17	53.72
Neplan	Flow [kg/s]	1.32	10.89	2.97	28.38	18.48	1.98	46.2	17.82	6.93	2.97	1.65
	Pressure drop [bar]	0.102	0.296	0.217	0.192	0.255	0.303	0.039	0.324	0.12	0.165	0.154
	T inlet [°C]	69.58	69.92	69.85	69.99	69.96	69.91	70.00	69.99	69.92	69.81	69.58
	T return [°C]	54.09	54.55	54.59	54.70	54.87	54.86	54.70	54.71	54.55	54.66	54.09

A relatively very small temperature difference is observed for all segments (less than 1.5%). For the flow and pressure drops, a relative error between 0.8% and 2% has been observed.

3.4. Validation with operating data from existing networks

The quantum network discretization methodology described in this study is implemented in the ADVENS network simulation tool. In addition to the quantum input parameters, the latter makes it possible to integrate:

- Effectiveness (ε) of heat exchanger and/or heat pump substations;
- Typical hourly load scenarios for domestic hot water (DHW) production in substations;
- Hourly temperature profile for the network environment.

Validation for this method is carried out based on a calibration process of the operating data of real existing networks operated by Groupe E: Low-Temperature DHC network with heat-pumps (TOUR-DE-PEILZ) and a High-Temperature DH network with heat exchangers (ESTACAD).

Low-Temperature DHC network with heat-pumps:

Figure X1 helps compare the energy data simulated by ADVENS with the operating/measured data of the existing LT district heating/cooling network described in section 3.1 (TOUR-DE-PEILZ). The coefficient of performance (COP) of the heat-pumps used at the substations in function with the temperature levels of the primary and secondary networks is taken from [Simon 2020].

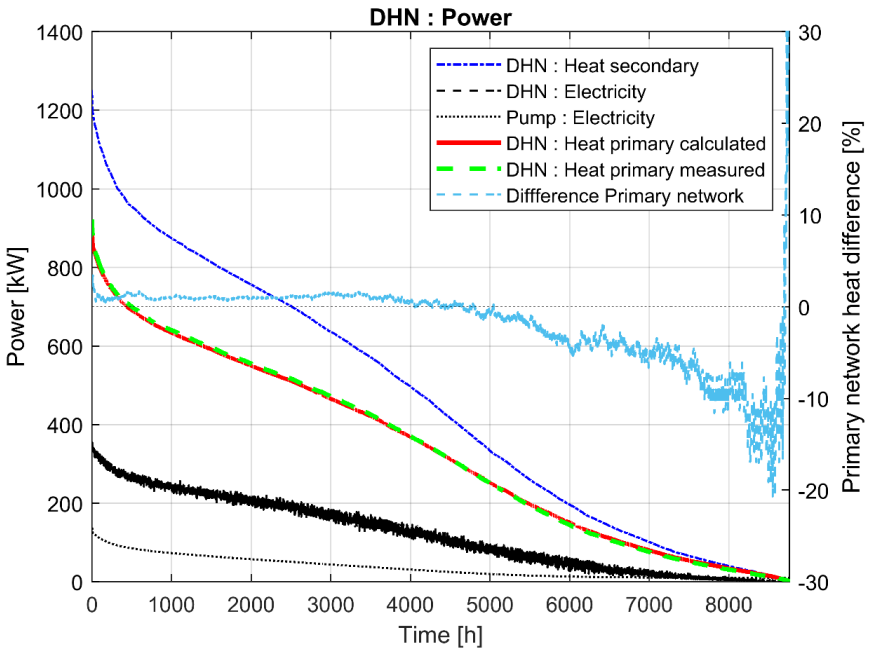

Figure X1 - Difference between the simulated data from ADVENS and the operating data from a 10°C-DHC system using heat-pumps at substations to provide heating and hot water in buildings (TOUR-DE-PEILZ)

Figure X1 represents the cumulated hourly evolution of the total energy demand measured at heat pumps condensers level (secondary network heat rate in blue in the graph); at evaporators level (primary network heat in discontinuous green): and it shows the electricity consumption of the heat pumps (in continuous black) and the circulating pumps of the pumping station (in discontinuous black). It also shows the relative difference (or deviation represented by the light blue curve) between the demand at the evaporators measured in the substations (in green) and that calculated by the ADVENS (in red):

In winter and between seasons – when demand variations in the secondary network range between 300 and 1'200 kW (up to 5'500 hours) – the deviation is stable and is very low (around 1%), and the primary network heat rates (200-900kW) calculated from the model are quite similar to those measured. It should be noted that, during the summer, the input data of the model, in particular the hourly load scenarios for domestic hot water (DHW) production, are not fully validated. Similarly, no thermal storage model has yet been implemented into the simulation. Thus, the average deviation

is of the order of 5%, corresponding to a demand between 60 and 200 kW in the secondary network (which represents approximately 5-16% of the nominal value). It is difficult to analyze the data below 5% of the nominal value, considering the low heat rates involved.

In total, out of the 2'929 MWh/y of energy measured in the primary network, a total energy of 2'918 MWh/y is simulated, and a difference of 11 MWh/y (equivalent to 0.4%) is therefore obtained. The small differences observed between the simulated data and the measured/operating data allow validation of the quantum network model.

High-Temperature DH network with heat exchangers:

Validation of the quantum network method is also carried out for a higher temperature level of network (ESTACAD at 85°C). This network includes 53 heat-exchanger substations that produce both heating energy for buildings and domestic hot water (DHW). The average altitude is 471m and the length of excavations correspond to ~3950m. The heating production plant capacity is 2,900 kW, with biomass boilers, and 2,600 kW with gas boiler. In fact, three biomass boilers of 500 kW, 1,200 kW and 1,200 kW respectively are available to cover the band load. A single 2,600 kW gas boiler is used as a heating backup during severe cold weather or as a backup when a biomass producer is out of order. The plant does not include a heat accumulator, the heat production is therefore constantly suited to the demand on the network.

Figure X2 makes it possible to compare the actual network operating curve data for the year 2019 with the data simulated by ADVENS.

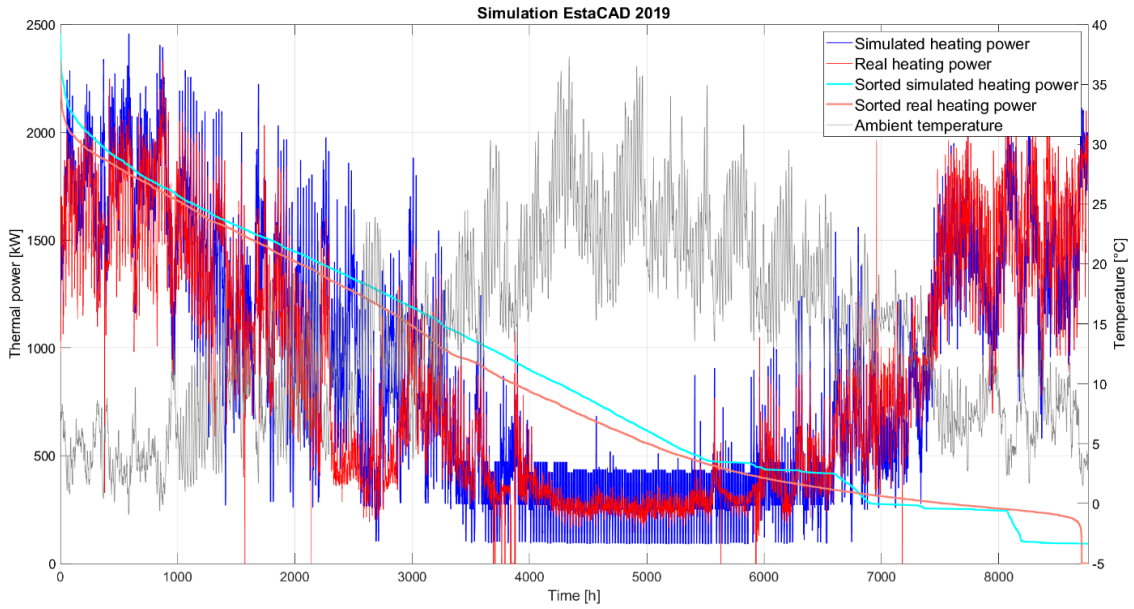

Figure X2 - Difference between the 2019 operating data from ESTACAD and the simulated data from ADVENS

The simulated data is obtained based on an atomic nucleus model composed of 53 protons (p=53) and 15 neutrons (n=15), which corresponds to a quantum network ($^{68}_{53}X$) of a maximum 31 branches or layers (l=2n+1=31) and 68 segments or sublayers (A=n+p=68). A very good correlation of hourly energy production curves (sorted hourly evolution of simulated and real measured heat rate) is observed. The network flow quantities are obtained for a network temperature difference ΔT of 15°C and a central supply temperature of 85°C. Network energy losses amount to 916.5 MWh/year, or 11.68% of annual production. In winter, these losses represent between 6% and 12% of the total energy produced. During the summer period, they average up to 30% of the energy produced.

4. The case study of BlueFACTORY DH network

The network of BlueFACTORY (called bluCAD) is an intelligent 4th generation DH network. Such a type of networks must be able to supply heating and cooling energy to all 12 customers while minimizing thermal losses (particularly when heating), to recycle heat from low-temperature sources

as well as hot water discharges, to integrate local renewable heat sources (geothermal, solar thermal, ambient air) into the network and, finally, to control and adapt production to the demand.

The DH network of the BlueFACTORY (BF) district in Fribourg illustrated by Figure 23 is able to provide a power of 3.2 MW at 80°C for an annual energy supply of 7700 MWh to thirteen consumers. The network reaches a length of 540 m through thirteen branches and six divergents. As the energy supplied is substantial in relation to the length of the network, it is a very high energy density network. The energy density value reaches 14.3 MWh/m.

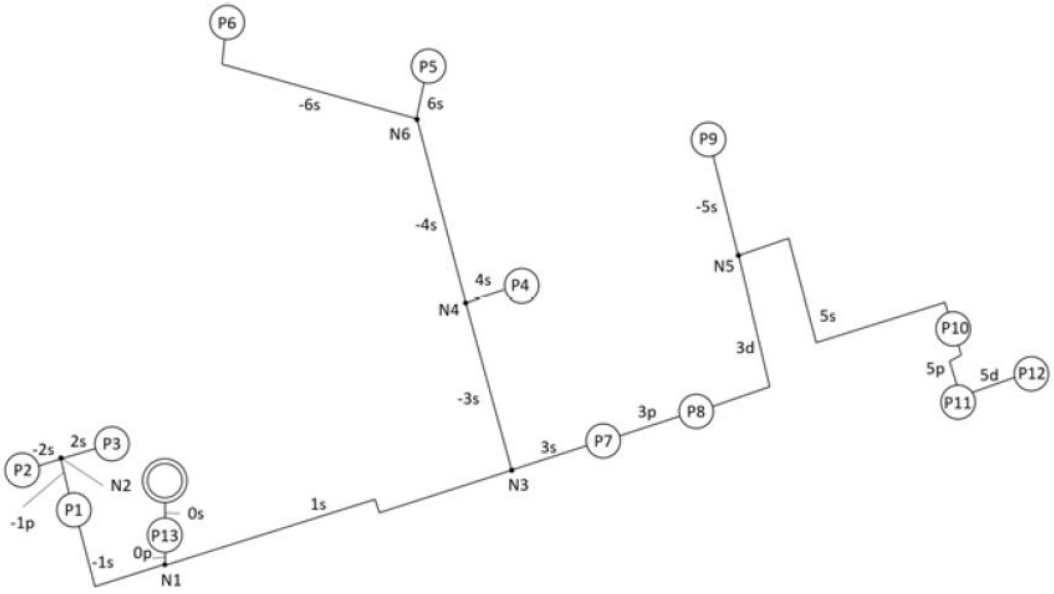

Figure 23: BlueFACTORY's DH network in Fribourg, Switzerland

These characteristics are clearly identifiable in figure 27a. Indeed, as the energy density is very high, the ratio of heat losses is much lower (0.6-6.4%) than the networks illustrated previously (density of 3.4-4.3 MWh/m). Another characteristic of a short DH network supplying energy to many consumers is that the singular pressure drops are preponderant over the linear losses as shown in Figure 24b.

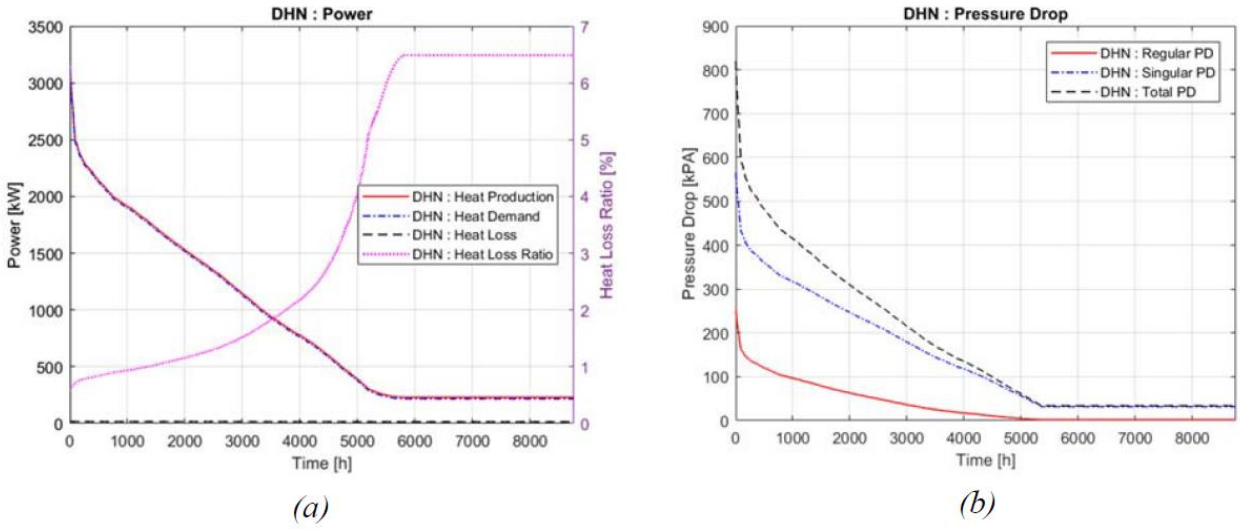

Figure 24: Characteristics of BlueFACTORY's DHN: a) DHN power, b) DHN pressure drops

This network is intended to welcome other users in the future. However, the plant capacity should not change drastically, since the objective is to reduce the network's temperature level to reach medium temperature levels (30-40°C). The buildings on the site will all be renovated; the lowering of the temperature level will not cause any problem and domestic hot water could be produced in a decentralized system or by heat pump in substation. As a result, it is expected that the system's energy efficiency will be significantly improved in future.

5. Conclusion

A new approach of cluster/layer-based "quantum network" modelling inspired by quantum mechanics is proposed to simulate, design and operate complex district heating/cooling systems with no iteration procedures. It consists of grouping together different substations, segments and/or branches into a network subsystem forming a cluster or an atom in the quantum network with its layers and sublayers. The atom is formed by a group of particles comprising a nucleus (primary circuit components) and electrons represented by the numerous substations distributed in the secondary circuit.

Based on this new formulation, the minimum quantity of flow transferred in a branch or segment of a network can be known in function of different parameters or quantum numbers (n, l, k, μ). Thus, the distribution of flow-energy in the branches and segments of any network could then be modelled

and simulated by using quanta (distribution of energy on the basis of discontinuous quantities): the flow-energy carried by any system or subsystem of the network is demonstrated to be a constant multiple (k_0) of a simple "quantum state function ν", the latter being characteristic of the studied system. The proportionality coefficient is the "k" factor of the network system, characterizing the production capacity per number of substations. In this context, modelling or simulating networks thus become much simpler to perform.

This method helps interpret and discretize any type of urban network. It has been applied to four different networks in order to demonstrate the robustness of the quantum network models and compare the performances of such networks. Validation of this method has been performed with a great accuracy of simulation results by comparing them to simulated data from a well-known commercial software (Neplan) and to real/operating data from existing DHC systems. A typical application for a set of high-performance buildings in the BlueFACTORY district (Fribourg, Switzerland) has also been considered to simulate different structures (branched, mesh or mixed network systems) of advanced thermal networks. Performances, in term of pressure drop and thermal losses on pipes, are determined on an hourly basis.

A real advantage of this cluster/layer-based quantum network design method is its flexibility, suitable both for use in an early design tool or for a new tool that engineers would use for detailed engineering design. Different networks at different levels of temperature can be interconnected and the expansion can be easily simulated to distribute energy to various zones or clusters (atoms or layers). A cluster can be a centralized or decentralized plant, a group of substations, branch/segment or any portion of the network. The simulation process of each cluster or layer can be carried out independently and in parallel in order to determine the flow-energy without any iterative procedures. New appropriate dimensionless key parameter indicators are defined and provided. Fast optimization process in a conceptual design and/or engineering design can be performed to compare various DHC systems options. Big data from existing DHC systems can be easily processed to analyze and predict the performances for good accuracy.

Highlights:

- Original method of cluster or layer-based design to model, simulate and operate district heating/cooling (DHC) system
- Novel formulation of distribution of energy in DHC networks using quantum numbers and appropriate dimensionless key parameter indicators
- Fast optimization process in a conceptual design and/or engineering design is proposed to compare various options of DHC systems
- Big data from existing / operating DHC systems can be easily processed to analyze and predict performances with great accuracy

Acknowledgements

References

[1] S. Werner, "International review of district heating and cooling," *Energy*, vol. 137, pp. 617–631, Oct. 2017, doi: 10.1016/j.energy.2017.04.045.

[2] H. Lund, N. Duic, P. A. Østergaard, and B. V. Mathiesen, "Future district heating systems and technologies: On the role of smart energy systems and 4th generation district heating," *Energy*, vol. 165, pp. 614–619, Dec. 2018, doi: 10.1016/j.energy.2018.09.115.

[3] H. Lund, B. Möller, B. V. Mathiesen, and A. Dyrelund, "The role of district heating in future renewable energy systems," *Energy*, vol. 35, no. 3, pp. 1381–1390, Mar. 2010, doi: 10.1016/j.energy.2009.11.023.

[4] H. Lund *et al.*, "Perspectives on fourth and fifth generation district heating," *Energy*, vol. 227, p. 120520, Jul. 2021, doi: 10.1016/j.energy.2021.120520.

[5] H. Lund *et al.*, "4th Generation District Heating (4GDH): Integrating smart thermal grids into future sustainable energy systems," *Energy*, vol. 68, pp. 1–11, Apr. 2014, doi: 10.1016/j.energy.2014.02.089.

[6] H. Li and S. Svendsen, "Energy and exergy analysis of low temperature district heating network," *Energy*, vol. 45, no. 1, pp. 237–246, Sep. 2012, doi: 10.1016/j.energy.2012.03.056.

[7] I. Sarbu, M. Mirza, and E. Crasmareanu, "A review of modelling and optimisation techniques for district heating systems," *International Journal of Energy Research*, vol. 43, no. 13, pp. 6572–6598, 2019, doi: https://doi.org/10.1002/er.4600.

[8] I. Ben Hassine and U. Eicker, “Impact of load structure variation and solar thermal energy integration on an existing district heating network,” *Applied Thermal Engineering*, vol. 50, no. 2, pp. 1437–1446, Feb. 2013, doi: 10.1016/j.applthermaleng.2011.12.037.

[9] C. Bordin, A. Gordini, and D. Vigo, “An optimization approach for district heating strategic network design,” *European Journal of Operational Research*, vol. 252, no. 1, pp. 296–307, Jul. 2016, doi: 10.1016/j.ejor.2015.12.049.

[10] R. J. Trudeau, *Introduction to Graph Theory*. Courier Corporation, 2013.

[11] B. Gumpert, C. Wieland, and H. Spliethoff, “Thermo-hydraulic simulation of district heating systems,” *Geothermics*, vol. 82, pp. 244–253, Nov. 2019, doi: 10.1016/j.geothermics.2019.07.001.

[12] S. A. Kalogirou, “Applications of artificial neural-networks for energy systems,” *Applied Energy*, vol. 67, no. 1, pp. 17–35, Sep. 2000, doi: 10.1016/S0306-2619(00)00005-2.

[13] A. Keçebaş and İ. Yabanova, “Thermal monitoring and optimization of geothermal district heating systems using artificial neural network: A case study,” *Energy and Buildings*, vol. 50, pp. 339–346, Jul. 2012, doi: 10.1016/j.enbuild.2012.04.002.

[14] H. V. Larsen, B. Bøhm, and M. Wigbels, “A comparison of aggregated models for simulation and operational optimisation of district heating networks,” *Energy Conversion and Management*, vol. 45, no. 7, pp. 1119–1139, May 2004, doi: 10.1016/j.enconman.2003.08.006.

[15] M. Vesterlund and J. Dahl, “A method for the simulation and optimization of district heating systems with meshed networks,” *Energy Conversion and Management*, vol. 89, pp. 555–567, Jan. 2015, doi: 10.1016/j.enconman.2014.10.002.

[16] B. Falay, G. Schweiger, K. O’Donovan, and I. Leusbrock, “Enabling large-scale dynamic simulations and reducing model complexity of district heating and cooling systems by aggregation,” *Energy*, vol. 209, p. 118410, Oct. 2020, doi: 10.1016/j.energy.2020.118410.

[17] J. Maria Jebamalai, K. Marlein, J. Laverge, L. Vandevelde, and M. van den Broek, “An automated GIS-based planning and design tool for district heating: Scenarios for a Dutch city,” *Energy*, vol. 183, pp. 487–496, Sep. 2019, doi: 10.1016/j.energy.2019.06.111.

[18] J. Wang, Z. Zhou, and J. Zhao, “A method for the steady-state thermal simulation of district heating systems and model parameters calibration,” *Energy Conversion and Management*, vol. 120, pp. 294–305, Jul. 2016, doi: 10.1016/j.enconman.2016.04.074.

[19] Y. Xu, C. Yan, H. Liu, J. Wang, Z. Yang, and Y. Jiang, “Smart energy systems: A critical review on design and operation optimization,” *Sustainable Cities and Society*, vol. 62, p. 102369, Nov. 2020, doi: 10.1016/j.scs.2020.102369.

[20] J. A. Wright, H. A. Loosemore, and R. Farmani, “Optimization of building thermal design and control by multi-criterion genetic algorithm,” *Energy and Buildings*, vol. 34, no. 9, pp. 959–972, Oct. 2002, doi: 10.1016/S0378-7788(02)00071-3.

[21] T. Fang and R. Lahdelma, “Genetic optimization of multi-plant heat production in district heating networks,” *Applied Energy*, vol. 159, pp. 610–619, Dec. 2015, doi: 10.1016/j.apenergy.2015.09.027.

[22] J. P. Abraham, E. M. Sparrow, and J. C. K. Tong, “Heat transfer in all pipe flow regimes: laminar, transitional/intermittent, and turbulent,” *International Journal of Heat and Mass Transfer*, vol. 52, no. 3, pp. 557–563, Jan. 2009, doi: 10.1016/j.ijheatmasstransfer.2008.07.009.

[23] C. T. GOUDAR and J. R. SONNAD, “Comparison of the iterative approximations of the Colebrook-White equation : Here’s a review of other formulas and a mathematically exact

formulation that is valid over the entire range of Re values : Fluid Flow and Rotating Equipment," *Hydrocarbon process. (Int. ed.)*, vol. 87, no. 8, pp. 79-83 [3 p.], 2008.